Abstract

Kelly Lake, located in the lowland of the Kenai Peninsula, Alaska, is a non-glacial, organic-rich, subaqueous spring-fed lake. A sediment core (KLY18-4) recovered from 4 m water depth offers multiple proxies including $d^{18}O_{marl}$ and $d^{13}C_{marl}$ values from ~14.1 to ~6.9 cal kyr BP, calcium carbonate content, magnetic susceptibility, and stratigraphic analysis to reconstruct lake level fluctuations, shifts in effective moisture, and precipitation source to the Kenai lowland from ~14.7 cal kyr BP to present.

The shallow-water macroalgae, *Chara* was likely the primary precipitating agent of calcium carbonate, or marl, at the core site from ~14.1 to ~6.9 cal kyr BP when lake level rose and the zone of marl production shifted to shallower water. Calcium carbonate content is used as a proxy for *Chara* growth and ambient water conditions as *Chara* prefers clear, shallow water.

Kelly Lake experienced overall lower lake levels and was likely a closed basin between the time of lake formation (~14.7 cal kyr BP) and ~6.9 cal kyr BP. Multiple shifts in lake level with periods of basin desiccation at the core site are also apparent during this time. The Younger Dryas exhibits cool and dry conditions at its onset but increasingly warm and evaporative conditions for its duration. The latter part of the Early Holocene shows an oscillatory pattern of lake level rise and fall and stepwise lake level rise beginning at ~7.5 cal kyr BP. Around 6.9 cal kyr BP the lake assumed relatively modern conditions with minimal subsequent fluctuation. Additionally, tephra deposits become more frequent here. Six deposits are found in the stratigraphy between ~6.9 cal kyr BP and present, and only one deposit is found between ~14.7 cal kyr BP and ~6.9 cal kyr BP. This suggests a potential shift to moisture sourced dominantly from the southwest bringing greater rates of precipitation and more ash fall from the Aleutian arc to the Kenai lowland.

Late Pleistocene and Holocene climate change on the Kenai Peninsula, Alaska: Interpretation of a marl record from Kelly Lake

By Emmy Wrobleski

A thesis presented to the Faculty of Mount Holyoke College in partial fulfillment of the requirements for the Degree of Bachelor of Arts with Honors

Department of Geology and Geography
Mount Holyoke College
South Hadley, Massachusetts

May, 2019

Advisor: Dr. Al Werner
Committee Members: Dr. Steve Dunn and Dr. Kate Ballantine
Department Chair: Dr. Steve Dunn

Acknowledgements

Firstly, I would like to thank my thesis advisor, Dr. Al Werner, for bringing me on the trip to Alaska to core Kelly Lake, introducing me to the paleoclimate research world, providing insight, and challenging me to consider multiple interpretations when I pined for one answer. Thank you to Ellie Broadman of Northern Arizona University for sampling for all the ^{14}C dates, constructing the age model, and providing interpretations and encouragement. Much gratitude towards Dr. Darrell Kaufman of Northern Arizona University and Dr. Don Rodbell of Union College for their expertise and insight, as well as to Dr. Rodbell's stable isotope laboratory for obtaining the $d^{18}O$ and $d^{13}C$ values and calcium carbonate content. Thank you to the University of Minnesota's LacCore facility where the cores were photographed and magnetic susceptibility obtained. Lastly, thank you to my mom, dad, big sister, and all my friends who provided words of encouragement and support throughout.

Whether eating ‘rittos in the cook tent,
Or coring all day,
Remember:
“Have alittle fun along the way!”

Table of Contents

List of Figures

List of Tables

1. INTRODUCTION

Numerous studies have been conducted to reconstruct past climatic and environmental changes on the Kenai Peninsula in south-central AK. This work has led to the development of multiple models of precipitation trajectory and source to the Kenai lowland (Bailey et al. 2015, 2019; Field et al., 2010; Jones et al., 2014, 2019; Kaufman et al., 2016; Schiff et al., 2008), and has established dates for certain climatic intervals and the general response of local lakes to environmental shifts (Abbot et al., 2010; Anderson et al., 2006; Jones et al., 2014, 2019; Kaufman et al. 2004; Kaufman et al., 2010; McKay and Kaufman, 2009; Yu et al., 2008;). To our knowledge, little research has been conducted on lakes in Alaska that contain calcium carbonate, or marl, deposits in their sediment record (Moxham and Eckhart, 1956).

Marl precipitates in temperate carbonate lakes primarily through biochemical processes. For marl to substantially accumulate in the lake deposits, the terrain surrounding the lake must have a low topographic relief, a precipitating agent, and appropriate physical and chemical conditions promoting precipitation of carbonates (Moxham and Eckhart, 1956). Precipitation of carbonates, namely calcite, is associated with photosynthetic processes of charophytes (*Chara*), a macroalgae that grows in the photic zone. The calcite forms as encrustations on the stem and thalli of the algae body, falls to the lake floor, and is preserved in the stratigraphic record. These deposits are used as a proxy for *Chara* growth which

is partially dependent on water clarity and depth (Winton et al., 2007; Pukacz et al., 2016; Apolinarska et al., 2011).

The marl deposits also reflect the carbon and oxygen isotopic composition of the ambient water at the time of formation. The $d^{13}C$ of the marl deposits ($d^{13}C_{marl}$) is reflective of the isotopic composition of dissolved inorganic carbon (DIC) in the water column which is affected by primary productivity in the lake and the isotopic composition of groundwater input (Anderson et al., 2005) The $d^{18}O$ of marl ($d^{18}O_{marl}$) reflects the oxygen isotopic composition of the water column which is affected by precipitation and evaporation (P-E) changes and the source of moisture.

This study aims to interpret the recent climatic history of the Kenai Peninsula and the responses of Kelly Lake to environmental changes from a ~6 m core from Kelly Lake, AK. This core contains marl deposits in the bottom half, providing a record of variations in the carbon and oxygen isotopic compositions of the ambient water at the time of marl formation from ~14.1 - 6.9 cal kyr BP. This record, accompanied by stratigraphic interpretation, calcium carbonate content, and magnetic susceptibility (used to define ash fall (tephra) layers), is used to reconstruct lake level fluctuation, shifts in effective moisture, and precipitation source to the Kenai lowland from ~14.7 cal kyr BP to present.

2. SETTING AND GEOLOGY

2.1 Study Area

Kelly Lake is a small, organic-rich kettle lake located in the Lowland of the Kenai Peninsula (Fig. 1.a) about 50 km east of Cook Inlet, 10 km west of the foothills of the Kenai Mountains, and about 7 km north of Skilak Lake (Fig. 1.b). It is situated 90 m above sea level at 60°30 N. Kelly Lake is one mile south of the Sterling Highway, where there is a small access road. Its surface area covers about 0.6 km^2 (U.S. Fish and Wildlife Service). The banks of the lake are shallow and populated primarily by birch and spruce trees. At its depositional center towards the west end of the lake, its depth reaches 12.5 m. The eastern end shallows gradually until it reaches a low bench with depths ranging from <1-5 m. The bottom deposits in this shallow basin are visibly lighter in color than the deposits from the depo-center. On satellite imagery, the lake bottom of this shallow part of the lake appears white (Fig. 2).

2.2 Hydrology

Having no inlet and only a small outlet stream on its western bank running into adjacent Petersen Lake located about 152 m to the west, Kelly Lake is currently classified as an open lake system. In the shallow, eastern basin (~0.5 - 2 m water depth) underwater springs provide a source of groundwater to the lake. About 610 m to the east at about 100 m elevation lies Hikers Lake, which is not

currently directly hydraulically connected to Kelly Lake, although these may be connected via groundwater flow.

2.3 Geologic Setting and Bicarbonate Source

The bedrock of the east side of the Kenai Mountains consist primarily of Mesozoic greywacke, while the west side facing the Kenai lowland consists primarily of Mesozoic metasedimentary rocks. Multiple Pleistocene glaciations of the Kenai deposited poorly consolidated to unconsolidated glacial till from the Kenai Mountains to the east of the lowland and from the southern part of the Alaska Range to the west of the Cook Inlet. These glacial Quaternary deposits are underlain by flat Tertiary-age sedimentary deposits of sandstone, siltstone, shale, and coal (Berg, unpublished, 2018).

Southwest of the Kenai Peninsula lie the Aleutian Arc, an active volcanic arc that stretches west from the Gulf of Alaska into the Bering Sea (Fig. 1.a). The Aleutian arc periodically sends ash plumes to the Kenai Peninsula which are deposited instantaneously as tephra layers in the lake sediment record.

The McHugh complex, weakly metamorphosed clastic and volcanic rocks Permian to Cretaceous in age located in the northwest flank of the Chugach Mountains on the Kenai Peninsula contains blocks of recrystallized limestone and marble lenses (Kusky et al., 1999; Clark et al., 1973). These calcium carbonate-bearing rocks may be present in the glacial drift surrounding Kelly Lake providing bicarbonate ions through groundwater input.

2.4 Climate and Vegetation

Climate

The Kenai Peninsula maintains a temperate boreal forest climate. Water vapor and precipitation from the Gulf of Alaska to the east of the Kenai Peninsula is obstructed by the Kenai Mountains, casting a rain shadow on the Kenai lowland. Mean annual rainfall and snowfall for the lowland between 1981 and 2010 was 46.25 cm and 171.45 cm, respectively. The mean annual temperature at the Kenai Airport was 2.3 degrees Celsius for the same timeframe (Alaska Climate Research Center, http://climate.gi.alaska.edu).

The Aleutian Low (AL), a semi-permanent low-pressure system off the coast of Alaska near the Aleutian Islands and the Bering Sea, influences local shifts in isotopic composition, amount, and seasonality of precipitation. Its strength and position changes on decadal timescales, characterized by the North Pacific Index (NPI; Trenberth and Hurrell, 1994), and is related to shifts in the Pacific Decadal Oscillation (PDO; Mantua et al., 1997). Moreover, the AL exerts a strong seasonal variation as it moves east of the Kenai Peninsula towards the Gulf of Alaska for the spring and summer months when it intensifies, and west of the Kenai Peninsula toward the Bering Sea for the fall and winter months when it weakens (Trenberth and Hurrell, 1994).

Vegetation

The lake is surrounded primarily by *P. glauca* (white spruce), *Betula papyrifera* (paper birch), and some tall grasses and shrub along the banks (Fig. 3). Evidence of current aquatic vegetation is limited. The shallow basin hosts few

macroalgae and no evidence of current *Chara* habitation was present at the time of core recovery (late June 2018). Some green microalgae blooms were visible directly above underwater springs in the shallow basin and are presumed to be minor myxophyceae (cyanobacteria) blooms that may currently be the primary precipitator of calcium carbonate in the lake.

2.5 Glacial History and lake formation

The last glacial maximum (LGM) occurred towards the end of the Pleistocene, about 26.5 to 19.0 thousand years ago (ka). At this time, ice sheets covered many of the high-latitude landmasses in both hemispheres, but the timing and expression of climate warming differs between the two. Antarctica experienced warming at around 17.0 ka, while the northern hemisphere experienced warming about 2,000 years later as defined by the Bølling Allerød warm period between about 14.7 and 12.9 ka. Following this, the northern hemisphere experienced an abrupt cool period between 12.9 and 11.7 ka called the Younger Dryas (YD). The climate warmed again in the northern hemisphere and generally experienced warmer conditions over the Holocene (11.7 ka to present), with the exception of the Little Ice Age (LIA; ~1400 AD to ~1900 AD).

The Cordilleran ice sheet made its final advance onto the Kenai Peninsula about 23.0 ka, during the Naptowne glaciation. During this advance, the Kenai Lowland was blanketed by ice advancing from the Kenai mountains to the east. Ice advancing from the west filled the Cook Inlet trough and reached the westernmost edge of the Kenai Peninsula (Reger et al., 2007). During the

deglaciation of the Kenai Lowland numerous kettles formed from ice block burial and meltout. Most of the kettles that formed here are now small kettle lakes.

Multiple minor readvances and/or stillstands occurring between ~23.0 and ~15.0 ka are evident by the morainal landscape in northcentral Kenai Peninsula. The ice made its second to last advance between ~17.5 and 16.0 ka during the Skilak Stade. Here, the ice margin advanced to a position just east of Kelly Lake and meltwater channels likely flowed through the lake and what is now the east fork of the Moose River (Reger et al., 2007). The ice made its final advance at ~15.0 ka during the Elmendorf Stade and meltwater channels ceased to pass through the current Kelly Lake locale. Subsequently, the kettle likely began to fill. The Naptowne Glaciation ended at ~11.0 ka after which glaciers on the Kenai Mountains remained at or behind present glacier margins.

3. PREVIOUS WORK

3.1 Late Pleistocene and Holocene environmental change on the Kenai Peninsula

Influences of the Aleutian Low on AK Climate

Much of the research on Quaternary environmental change on the Kenai Peninsula emphasizes the role of the AL as it has a strong seasonal influence on the isotopic signature, amount, and seasonality of local precipitation. During the winter and early spring, the AL strengthens, shifts just west of the Kenai Peninsula, and remains there for the remainder of the summer delivering higher $d^{18}O_{precip}$ values to the Gulf of Alaska (Bailey et al., 2015; Kaufman et al., 2010; Field et al., 2010). In late summer, the system splits in two; one center resides west of the Bering Sea, and the other east of the Kenai in the Gulf of Alaska. The system remains here for the winter, delivering isotopically lighter precipitation to the Kenai lowland from the northeast (Bailey et al., 2015).

During periods of strengthened AL, the Kenai Peninsula receives more storms from the southwest, increasing precipitation and warm moist air during the winter months. Kaufman et al. (2010) found that in Homer, AK (120 km southwest of Kelly Lake) winter precipitation is negatively correlated with the North Pacific Index (NPI) which has an inverse relationship to the strength of the AL (Mantua et al., 1997; Trenberth and Hurrell, 1994). This suggests that Anchorage and potentially the Kenai lowland to the south experience greater precipitation rates during strong AL winters.

However, Bailey et al. (2019), a modern isotope study conducted in Anchorage, AK (80 km north of Kelly Lake), did not find a statistically significant relationship between their Anchorage $d^{18}O$ dataset from 2005 to 2018 and the North Pacific Index (NPI), the Pacific-North American, nor the Pacific Decadal Oscillation (PDO), all related to the strength and position of the AL. A limitation to this study is the short time series used to correlate changes in isotopic signature of precipitation and the abovementioned climate indices. They did however, find that when a low-pressure center resided over the Kenai Peninsula, storms tracked from the north and the peninsula experienced the lowest winter $d^{18}O$ values. When a low-pressure center resided just west of the peninsula, storms tracked from the south and winter precipitation was enriched in ^{18}O. Bailey et al. (2019) also observe a strong seasonal variation in isotopic signatures of precipitation. Anchorage experienced higher mean $d^{18}O$ values during the summer (-14.4‰) and lower values in the winter (-19.6‰) months. During the spring and summer months, more storms track from the south bringing isotopically heavier precipitation to the peninsula. Conversely, more storms track from the north during the winter months lowering the isotopic signal of precipitation on the Kenai. Although they do not argue that this shift in storm track direction is a result of shifting AL pressure centers, their findings are consistent with previous studies that have suggested the position of the AL as the primary driver of $d^{18}O_{precip}$ change (Jones et al., 2019 and 2014; Anderson et al., 2005, Schiff et al., 2008; Bailey et al., 2015).

Major Climate Intervals

Warmer intervals such as the Bølling Allerød (14.0-12.9 ka) and the Holocene Thermal maximum (HTM; 11.0-9.0 ka) expressed in Alaska are reported to be associated with relatively higher (more positive) $d^{18}O$ values, while cooler intervals such as the Younger Dryas (12.9-11.7 ka) are associated with lower (more negative) $d^{18}O$ values (Jones et al., 2014). Jones et al. (2014) associates heavier isotopic signals during warmer climate regimes to a strengthened AL and enhanced effective moisture. They associate the lighter isotopic signals during the cooler regimes to a weaker AL and drier conditions.

The Bølling Allerød warming period brought the Kenai Peninsula out of the Naptowne glaciation at around 14.0 ka. This interval coincides with rich fen conditions and high $d^{18}O$ values, as observed at Horse Tail fen by Jones et al. (2014 and 2019).

Kaufman et al. (2010) explores the expression of the Younger Dryas in south-central Alaska at Discovery Pond (DP), about 30 km northwest of Kelly Lake on the Kenai Peninsula. Their records suggest that prior to the onset of the YD, a fen developed at their site. At the onset of the YD (around 12.8 ka) they conclude that climate conditions in the Kenai Lowland were colder and drier as evidenced by reduced lake productivity. Their records show a shift in microfossil assemblage at around 12.2 ka which indicates increased lake depth presumably caused by elevated effective moisture. They suggest that late YD warming continued into the early Holocene and its peak may coincide with the maximum summer insolation at 65 degrees N latitude. Furthermore, they attribute a

strengthening and eastward position of the AL (west of the Kenai) to the rise in effective moisture at the study site. Kaufman et al. (2010) compiled evidence of similar YD warming trends in other records from south-central Alaska and greater Beringia. In south-central Alaska, records from Hundred Mile Lake (Yu et al., 2008) and Greyling Lake (McKay and Kaufman, 2009) exhibit overall increases in organic matter throughout the YD. In the northwest Pacific Ocean (core MD01-2416; Sarnthein et al., 2006), southwest Alaska (Arolik Lake; Hu et al., 2006), and the Gulf of Alaska (core EW0408-85JC; Barron et al., 2009), $d^{18}O$, BSi, and organic matter records yield evidence for warming trends during this time.

Conversely, most YD records exhibit evidence for cool and dry conditions for its duration. The Greenland Ice Sheet Project provides a $d^{18}O$ record from Greenland ice cores. This record exhibits low $d^{18}O$ values for the duration of the YD suggesting cold conditions. This interval however, is likely expressed differently on the Kenai Peninsula than in Greenland. Jones et al. (2014 and 2019) examine a peat core taken from Horse Trail Fen, about 30 km west-southwest of Kelly Lake. This analysis of microfossil assemblages and oxygen isotopes suggests cold and dry conditions with little variance in temperature and effective moisture for the entire YD until 11.5 ka. Jones et al. (2014) attributes this to a strengthened and eastward AL and enhanced orographic uplift after interpretations of the Jellybean Lake record in Yukon, Canada by Anderson et al. (2005) who suggests a negative correlation between $d^{18}O$ values and AL strength. However, the sign of this correlation was incorrectly reported by Anderson et al. (2005) and this record actually exhibits a positive correlation between $d^{18}O$ values

and AL strength (Kaufman et al., 2016). These records therefore suggest a weakened AL for the duration of the YD resulting in cool and dry conditions.

High accumulation rates of well-preserved peat during the early Holocene (beginning ~11.7 ka) have been attributed to warm and wet conditions on the Kenai Peninsula (Jones et al., 2009 and 2014; Jones and Yu, 2010). Jones et al. (2019) uses $d^{18}O$ from the cellulose of plant remains in a peat core from Horse Trail Fen on the Kenai lowland as a proxy for environmental change. These records show lower $d^{18}O$ values between 11.7 and 10.8 ka. They attribute this shift to rising sea levels and greater sea ice extent and potentially increased winter precipitation with lower $d^{18}O$ values and enhanced long-range transport. In contrast, Kaufman et al. (2010) find a decrease in effective moisture on the Kenai during the early Holocene, starting at 11.0 ka. A dense peaty mud layer formed between 10.8 and 9.8 ka is interpreted as deposited in very dry conditions and coinciding with the Holocene Thermal Maximum (HTM). Drier conditions and lower lake levels between 9.5 and 8.0 ka are also reported in Anderson et al. (2006) which analyzed records from Arrow and Portage Lakes located in the northwest part of the Kenai Peninsula. Kaufman et al. (2016) analyzed midge abundance as a proxy for summer temperatures in eastern Beringia (which includes Alaska, westernmost Canada, and adjacent seas) over the Holocene. Their composite midge record exhibited evidence for highest summer temperatures (HTM) during the early Holocene (10.0-9.5 ka) and minor cooling during the late Holocene. They suggest that the HTM began on the Kenai Peninsula at around 10.0-11.0 ka, and ended at around 9.0-10.0 ka.

The Horse Trail Fen peat core record analyzed in Jones et al. (2014) suggests drier conditions 8.5-1.6 ka based on a decrease in peat preservation and increased charcoal abundance. Conversely, a shift to cool and wet conditions at 8.0 ka resulting in lake level rise has been reported as a trend across the western Arctic (Kaufman et al., 2004), in central Alaska (Abbot et al., 2000), and in southcentral Alaska (Yu et al., 2008).

Anderson et al. (2005) used lacustrine carbonate isotopes from Yukon Territory to reconstruct regional atmospheric circulation change during the Holocene. Their marl record ends around 7.5 and they attribute this to a shift to modern lake conditions.

3.2 Marl deposition in freshwater lakes

Deposition of marl in hard-water lakes occurs through physiochemical processes and is common in temperate regions with local glacial drift. Temperate marl lakes do not occur above 150 m elevation, nor north of 60 degrees' latitude (Kindle 1927, 1929 in: Murphy and Wilkinson, 1980).

The accumulated lake deposits must have a high enough ratio of calcium carbonate to be considered marl. Typically, 25% calcium carbonate is considered the lower limit for marl classification. Samples yielding lower percentages are classified as calcareous silt (Pettijohn, 1949 in: Moxham and Eckart, 1956).

The two most common carbonate precipitating agents in temperate lakes include charophytes and myxophyceae (Moxham and Eckhart, 1956; Bathurst, 1975; Welch, 1935). Charophytes are distinctive fresh- and brackish-water

bottom-rooted macroalgae closely resembling aquatic plants and belonging to the family, *Characeae*. Dependent on sunlight to photosynthesize, they reside in the littoral zone (1-3 m water depth) in clear, alkaline waters with low nutrient input rates (Winton et al. 2007, Pukacz et al., 2016). Their occurrence is indicative of low trophy and high ecological status (Apolinarska et al., 2011). Charophytes utilize bicarbonate molecules in the water column as a primary source of carbon to carry out photosynthesis during which a micro-environment of elevated pH immediately surrounds the algae inducing calcium carbonate precipitation on its thalli and stems. Myxophyceae grow in blooms and are shown to mediate the precipitation of calcite in freshwater environments (Bathurst, 1975; Welch, 1935)

3.4 Charophyte responses to environmental change

Modern *Chara* studies such as Rip et al. (2007) report that in years with increased precipitation and runoff, higher levels of phosphorus input resulted in algal blooms and increased light attenuation. Additionally, with increased precipitation and runoff, large amounts of humic acids (dissolved organic substances) were washed into the lake further increasing light attenuation. Due to the resulting decrease in water transparency, *Chara* populations declined. However, in years with less precipitation, *Chara* populations grew and remained stable.

3.5 $d^{18}O$ and $d^{13}C$ isotopes from marl deposits as proxies for environmental change

Carbon and Oxygen Isotopes

Pentecost et al. (2006) reports substantial isotopic disequilibrium between $d^{13}C$ and $d^{18}O$ of carbonates and that of ambient waters when charophytes were subject to extreme conditions such as rapid lake level fall during the growing season. *Chara*-precipitated marl deposits are found to be depleted in both ^{13}C and ^{18}O (more negative $d^{13}C$ and $d^{18}O$ values) with respect to the ambient water (Pentecost et al., 2006; Pronin et al., 2018). Despite this disequilibrium, Pelechaty et al. (2010) finds correlation between $d^{13}C$ and $d^{18}O$ of carbonate encrustations and $d^{13}C$ and $d^{18}O$ of ambient waters. These signals can therefore serve as proxies for the isotopic composition of the ambient water at the time of carbonate formation. Anderson et al. (2005) also found *Chara* encrustations precipitating in approximate equilibrium in a closed, spring-fed carbonate lake in south-central Yukon.

Carbon

$d^{13}C_{marl}$ values are reflective of primary productivity in the lake. During the growing season, preferential uptake of ^{12}C during photosynthesis elevates the $d^{13}C$ values of the DIC in the water column (Leng and Marshall, 2004). Isotopically lighter values may also be indicative of changes in hydrology and incorporation of lighter CO_2 from decaying plant matter in soils and within the lake. Groundwater is typically isotopically lighter with depleted $d^{13}C$ values of –10‰ to –15‰, while atmospheric exchange of CO_2 through mixing and

photosynthesis results in isotopically heavier DIC and higher $d^{13}C$ values in the sediment record (Anderson et al., 2005).

Chara-precipitated carbonates are found to be in isotopic disequilibrium with ambient waters. Encrustations may become enriched in ^{13}C relative to the isotopic composition of DIC due to photosynthesis preferentially utilizing the lighter isotope (Andrews et al., 2004; Coletta et al., 2001; Pelechaty et al., 2010). Additionally, higher $d^{13}C$ values in the marl may be caused by the mechanism of active transport used by *Chara* to utilize HCO_3^- in the water column for photosynthesis. This complicates photosynthetic fractionation of carbon and results in enrichment of $d^{13}C$ values of calcite (Diefendorf et al., 2007). If there are no major changes in primary precipitating agents in the lake, such as a shift from *Chara*-precipitated calcite to myxophyceae-precipitated calcite, the influence of active transport on the $d^{13}C$ values is likely not important.

Oxygen

If the lake is an open basin, the oxygen isotope composition of the marl ($d^{18}O_{marl}$) reflects the isotopic composition of precipitation ($d^{18}O_{precip}$) that is influencing the composition of the water column. If the lake is a closed basin, $d^{18}O_{marl}$ values reflect the precipitation-evaporation (P-E) signal that affects lake level and subsequently the $d^{18}O$ composition of the water column. If there is an evaporative influence on the lake, a drier climate would likely result in a heavier isotopic signal (more positive $d^{18}O$ values) as the lighter isotope is preferentially evaporated out of the water column. Consequently, a lighter isotopic signal (more

negative $d^{18}O$ values) would imply greater rates of precipitation and freshening of the lake water.

Although depletion in $d^{18}O$ of encrustations relative to the $d^{18}O$ of the ambient water has also been reported, it has been suggested that $d^{18}O$ analysis is a more reliable proxy for environmental change since it is less influenced by photosynthetic activity (Andrews et al., 2004; Coletta et al., 2001; Anderson et al., 2005). Although the literature discussed above suggests that higher $d^{18}O$ values are indicative of a strengthened AL and increased moisture from the southwest, and lower $d^{18}O$ values are reflective of a weaker AL and winds advecting from the northeast, many of these records are not from *Chara*-precipitated marl. It is therefore important to consider how disequilibrium between the isotopic values of the marl and those of the ambient water affect climatic and environmental interpretations. When storms track dominantly from the southwest, the Kenai lowland experiences an increase in precipitation which should effectively enrich the water column of closed basin lakes in the lighter oxygen isotope. Because *Chara* will precipitate marl depleted in ^{18}O, the isotopic signals of closed basin lakes will represent shifts in P-E, but not the exact isotopic composition of the water column at time of formation.

4. METHODS

4.1 FIELD METHODS

4.1.1 Core site selection

Core site #4 (N60.51444° W150.37372°) was chosen for its intermediate water depth (4 m) between the deep basin and the shallower, eastern basin of the lake. Furthermore, on Google Earth images (Fig. 2), the easternmost arm of Kelly Lake appears white, indicating the presence of marls in shallow water depths. As such, a water depth of four meters is considered shallow enough to likely have a rich marl record since marl is only deposited in shallow water depths, yet deep enough to not exhibit depositional hiatuses due to lake level fluctuations. The core site is currently located about 430 m west of the underwater springs.

4.1.2 Livingstone coring

We used Livingstone coring methods to recover core KLY18-4A. We recovered the core in one-meter-long segments until we bottomed out in glacial clays that the Livingstone corer could not penetrate. The cores were extruded from the device into a split-pipe, the pipe was packed with stiff, grey foam to secure the mud, taped shut, and labeled with the core site and core section number.

4.1.3 Surface coring

Because the Livingstone coring method does not reliably preserve the poorly consolidated core top we also recovered a surface core (KLY-18-4B-1U)

using a Uwitec coring device to capture the sediment-water interface. In the field, we suctioned the water off the top of the core tube and used Zorbitrol to absorb any water left on the top of the core. We packed the empty spaces in the core tube with florist foam, and capped and taped it to secure the mud for shipment to the LacCore core lab in Minnesota.

4.2 LABORATORY METHODS

All core splitting, photography, bulk density, and magnetic susceptibility was conducted at the LacCore facility at the University of Minnesota, Twin Cities. All chronology and sub-sampling were conducted at Northern Arizona University's Sedimentary Records of Environmental Change Lab. Coulometry and isotope analysis was conducted at Union College's Laboratory for Sediment Core Analysis by lab assistants and undergraduates there. Marl identification and XRD analysis was carried out at Mount Holyoke College's Microscopy Facility by Abby Boak, MHC '20.

4.2.1 Core Splitting/Photography

The surface core tube was cut with a cast saw, split vertically with a wire, and cleaned. Pre-split pipes housed the Livingstone cores, so no pipe-cutting was needed. We used wire to vertically cut each section of KLY18-4 and a glass microscope slide to clean the newly-cut surface. Each one-meter-long core segment was photographed using the Geotek Geoscan-III, a high-resolution line-scan CCD camera (Fig. 4)

4.2.3 Magnetic Susceptibility

Prior to splitting the cores, the Geotek MSCL-S loop sensor took automated continuous density measurements (g/cc) for each whole core segment. After the cores were split and photographed, the Geotek MSCL-XYZ point sensor (Fig. 5) took automated continuous magnetic susceptibility measurements (SI) every half centimeter for each split core segment.

4.2.4 Core Chronology

Six plant macrofossils were originally obtained from core KLY18-4. Fossils were selected throughout the core from sections KLY18-2, -3, -4, -5, and -6, roughly equidistant from each other. Full pretreatment on the macrofossils was performed using acid-base-acid procedure at Northern Arizona University by Ellie Broadman. After pretreatment the samples were sent to the W.M Keck Carbon Cycle Accelerator Mass Spectrometer at the University of California Irvine for AMS radiocarbon age assessment. The *Bacon* program in RStudio was used to reconstruct Bayesian accumulation histories and to calibrate the radiocarbon ages to produce an age model for the entire core. *Bacon* calibrated the radiocarbon dates using IntCal13 for terrestrial northern hemisphere material (Reimer, 2013). The sediment accumulation rate in the lake was modified at the depths where tephra layers are deposited.

4.2.5 Tephra Identification

Tephra deposits were identified based on their distinct magnetic susceptibility (MS) peaks and their lithostratigraphy. Tephra MS was

characterized primarily by singular MS peaks. Units with multi-peaked or complex high MS were not identified as a distinct tephra deposits but rather, sandy, clastic deposits. Prominent tephra deposits with known ages, such as the Hayes (3660 cal yr BP (deFontaine, 2007) to 4140 cal yr BP (Riehle et al., 1990)), were used to correlate and test the age model.

4.2.6 Subsampling

We subsampled KLY18-4A every centimeter for the first 293 cm core depth and starting at 8.5 cm core depth, and preferentially sampled marl deposits or prominent stratigraphic units every half centimeter for the remaining 327 cm, totaling 782 samples. The surface core, KLY18-4B, was sampled every half centimeter for the first half of the core (0.5 cm to 29 cm core depth) and every centimeter (30 cm to 57 cm core depth) totaling 86 samples. For many of the Livingstone core sections, the mud had shifted or shrunk slightly so the newly measured section depths did not concur with the recorded section depths when the cores were initially split. To reconcile this, we re-measured the core sections and added or deleted centimeters in the dataset. The samples were cut and scooped out of the core using a lab spatula, and placed in a small glass vial labeled for the section number of the core and the section depth (cm) of the sample.

4.2.7 X-Ray Diffraction (XRD)

Samples from throughout the core of the purest marl were selected for XRD analysis to determine the polymorph of calcium carbonate. Marl from sample ID numbers 3-1, 4-9, 4-52, 4-75, 5-21.5, 5-45, 5-73, 5-99, 6-25, 6-48, 6-

66, 6-86, 7-46, and 7-56.6 were used for analysis. Marl was smeared on glass slides and analyzed using the X-Ray Diffractor.

4.2.8 Coulometry

To measure percent $CaCO_3$ and percent total inorganic carbon (TIC), 51 samples were analyzed from the core using coulometry at Union College. Samples were treated with H_2O_2, wet-sieved through a solid-bottom 75 um sieve, decanted and centrifuged to isolate the sediment from the water. The samples were then bleached, freeze-dried for 36 hours, homogenized, and weighed. All negative numbers were deemed insignificant noise where measurements were so close to zero that they were beyond detection limits. Therefore, all negative measurements were replaced with zeros.

4.2.9 Oxygen and Carbon Isotopes

Isotope ratio mass spectrometry (IRMS) was conducted using a Thermo Gas Bench II connected to a Thermo Delta Advantage mass spectrometer. Samples were prepared for analysis using a custom manifold. Eighty ug of each sample was placed at the bottom of an exetainer vial, and about 40 uL of acid was pipetted into the neck of the vial avoiding contact with the carbonate. The vials were capped, pushed on the needles of the manifold, and cleaned with He gas at ~100 mL/min for 10 minutes. The heated block was added and the acid reacts with the carbonate at the bottom of the vial. Samples were then loaded into the Gas Bench II and analyzed for carbon and oxygen isotope ratios (Union College Stable Isotope Laboratory: http://minerva.union.edu/gillikid/lab.htm).

For isotopic corrections and to assign the appropriate isotopic scale to the data using linear regression, reference standards LSVEC, NBS-18, and NBS-19 were used. The following reference standard values were used for $\delta^{13}C$ and $\delta^{18}O$ respectively: LSVEC: -46.6‰, -26.7‰; NBS-18: -5.014‰, -23.2‰; and NBS-19: +1.95‰, -2.2‰. Based on 4 NBS-19 standards over 1 analytical session the analytical (combined) uncertainty for $\delta^{13}C$ and $\delta^{18}O$ are ± 0.02‰ (VPDB) and ± 0.04‰ (VPDB), respectively (Union College Stable Isotope Laboratory; Rodbell, pers. com.)

4.2.10 Carbonate Precipitating Agent Identification

To determine the source of the marl, we observed wet samples under a microscope to identify evidence of macrofossils such as *Chara* oospores or ostrocodes. Sixteen samples from various depths throughout the marl record (ID numbers 3-1, 4-9, 4-52, 4-75, 5-21.5, 5-23, 5-45, 5-71, 5-73, 5-99, 6-25, 6-48, 6-66, 6-86, 7-40, 7-56.5) were evaluated for *Chara* oospores. Samples were disaggregated in a shallow, white dish with deionized water and observed under a microscope for oospore abundance

4. RESULTS

We assume nearly full recovery based on the glacial clay basal sediments and the basal age that is consistent with the retreat of the ice from the study area. The short surface core (KLY18-4B) recovered from the same core site as the Livingstone core (KLY18-4A) captures the sediment-water interface and was used to complete the sediment record of the long Livingstone core. Near-identical sediment layers and magnetic susceptibility peaks from the short and long cores aided in correlating the two (Fig. 6). Based on the correlation, the long core includes the complete stratigraphic sequence except for the top 8 cm of the record.

5.1 Lithostratigraphy

Calcium carbonate ($CaCO_3$) was absent for the top 293 cm of the core where the stratigraphy is dominated by loose, organic-rich mud (Fig. 6). Percent $CaCO_3$ remains between about 36% and 84% for the bottom 327 cm. Differences in stratigraphic character reflect differences in $CaCO_3$ content (Table 1, 2). Higher $CaCO_3$ content is characterized by samples of pure, white to yellow, spongey marl deposits (n = 6: min = 68.2%; max = 84.0%; mean = 75.9%). $CaCO_3$ values reflected in light-brown, non-layered marl mud (n = 6: min = 58.9%; max = 75.5%; mean = 68.9%) and in yellow marl with faint to strong laminations of organic-rich material (n = 9: min = 59.3%; max = 80.4%; mean = 67.6%) are found to be approximately the same. Lower $CaCO_3$ values are found in the oldest sample tested, clay mixed with marl and organic material (n = 1: 63.0%).

Medium-brown marl mud (n = 3; min = 42.2%; max = 67.8%; mean = 57.6%) and organic material roughly evenly layered with yellow marl (n = 2: min = 50.3%; max = 53.4%; mean = 51.9%) have roughly half $CaCO_3$, and half non-calcareous material. Dark gray to brownish-gray, un-layered marl mud presumably have higher concentrations of terrigenous material and have lower $CaCO_3$ content (n = 2: min = 35.9%; max = 50.0%; mean = 43.0%). Lastly, one sample of dark organic matter with flecks of yellow marl dispersed throughout revealed low $CaCO_3$ content (n = 1: 36.1%).

5.2 Core stratigraphy

The composite core (KLY18-4) totaled 636 cm and is divided into 6 major units (Fig. 6). From bottom to top, the units include: (1) a 30 cm-thick basal layer of dense, inorganic, gray mud interbedded with some thin layers organic-rich brown mud and yellow to white spongy marl (calcium carbonate-rich mud) (590-620 cm core depth); (2) 80 cm of mostly pure marl of varying colors (light gray, yellow, and white) laminated with thin, medium-dark brown organic-rich mud (500-590 cm); (3) 35 cm of medium-grey marl with low CaCO3 content (475-501 cm); (4) 123 cm of marl or varying purities and colors (white, yellow, light brown) interbedded with thicker (~1-2 cm) and laminated with thin (~0.5-1 mm) layers of medium-brown mud (352-475 cm); (5) 68 cm of medium-brown organic-rich mud interbedded with four thick (1.5-2 cm) peat layers, each topped with thick (1-3 cm) layers of impure brownish- yellow marl (284-352 cm); (6) and 284 cm of medium-brown, organic-rich, loose mud with very low $CaCO_3$

content, plentiful herbaceous plant material (0-284 cm). Units 2 and 4 also contain *Chara* oospores (Fig. 7) dispersed throughout the marl units.

5.3 Age model

Six macrofossils were extracted from the core to produce an age model and assign ages to prominent stratigraphic units. Four produced useful radiocarbon ages (sample numbers 2, 4, 5, and 6; Table 3). Sample 1 (104 cm BLF) did not have enough carbon to graphitize and yield an age, and sample 3 (295 cm BLF), an aquatic plant leaf stem, yielded an unrealistic age of 11715 BP (uncalibrated). This sample was the only aquatic plant of the four age-yielding samples which were all from terrestrial plants (Table 2). It is likely that this aquatic plant incorporated "old carbon" (i.e. a hard water effect), which is a common occurrence in carbonate lakes (pers. com. Ellie Broadman). The age model resulted in a linear trend with no hiatuses and a calculated average sedimentation rate of 0.42 mm/yr. The model yielded a basal date of 14761 cal yr BP (Fig. 10).

5.4 Tephra Stratigraphy

Tephra deposits in KLY18-4 were less prominent than those in other lakes studied on the Kenai Peninsula and in south-central Alaska (Daigle and Kaufman, 2009; deFontaine, 2007). However, the cores from the depo-center, KLY18-1 and -2, exhibited numerous large peaks in MS, consistent with other lake records in the area. The nature of these tephra deposits in KLY18-4 can likely be attributed to the depositional environment at the time. This shallow basin likely housed aquatic plants which potentially disrupted direct deposition of the tephra, while

the deeper basin had little vegetation in its water column that could complicate tephra deposition.

Throughout the core, six tephra layers can be identified from their distinct peaks in MS and their lithostratigraphy. Although there are other prominent peaks in MS, they are less characteristic of volcanic ash deposits due to their multi-peaked nature (tephra layers often have one uniform peak.) These small, grainy units also contain broken-up organic matter, possibly indicative of storm or flood events. The tephra layers are identified as follows from the core base: (T1) ~0.5 cm of dense and prominent black-grained tephra deposit at 469 cm core depth and an age of about 11317 cal BP; (T2) 3 cm of fine, gray material with an age of 6152 cal BP (243.5-246.5 cm core depth); (T3) 2 cm of fine, grayish-brown material difficult to distinguish in the stratigraphy but with a distinct MS peak and an age of 5165 cal BP (210.5-212.5 cm core depth); (T4) a thick (~2 cm) pinkish-grey tephra layer with an age of about 4180 cal BP (171.5-173.5 cm core depth). This deposit is consistent with the age (3660 cal yr BP (deFontaine, 2007) to 4140 cal yr BP (Riehle et al., 1990)) and description of the well-known Hayes tephra in the literature; (T5) 3 cm of fine, grayish-brown material difficult to distinguish visually but with a distinct MS peak and an age of about 1978 cal BP (86.5-88.5 cm core depth); (T6) about 3 cm of fine, yellowish-gray material with a distinct MS peak and an age of about 465 cal yr BP (27-29 cm core depth).

5.5 X-Ray Diffraction (XRD) analysis

X-Ray Diffraction (XRD) analysis revealed that the marl deposits are composed of the calcium carbonate polymorph, magnesium calcite (Fig. 8).

5.6 Oospore identification

Chara oospores were found in the marl deposits (Fig. 7). Sample 5-21.5 (core depth = 405.5 cm) yielded 9 oospores, 5-45 (core depth = 430 cm) yielded 2, 5-73 (core depth = 457 cm) contained 31, 7-40 (core depth = 582 cm) contained 1, and 7-56.5 (core depth = 598.5 cm), 2.

5.7 Total inorganic carbon (TIC)

Inorganic carbon exists dissolved (DIC) in the water column largely as carbon dioxide (CO_2) and bicarbonate (HCO_3^-). Generated by myxophyceae, algae, and other plants both within the lake and its surrounding catchment, these organic compounds serve as the primary source of carbon for photosynthesis in a lake (Wetzel, 2001).

Total inorganic carbon (TIC) values analyzed in the 30 samples containing $CaCO_3$ tracked closely with their respective $CaCO_3$ content (Fig. 6). Percent TIC ranged from 4.3% to 10.1% for the samples containing $CaCO_3$. Percent TIC was 0% for the samples not containing $CaCO_3$.

5.8 Oxygen isotopes

The $d^{18}O_{marl}$ values derived from analysis of the 51 samples containing sufficient $CaCO_3$ differ by up to 3.99‰ between 604 and 276.5 cm below lake

floor (BLF; Fig. 9). The lowest value reached -17.39‰ at 293 cm BLF, while the highest value reached -13.59‰ at 505 cm BLF. The first value at 604 cm BLF yields a $d^{18}O_{marl}$ value of -14.43‰. $d^{18}O_{marl}$ decreases to -15.62‰ at 588 cm BLF and then proceeds to increase gradually until 555 cm BLF where it reaches -14.43‰. $d^{18}O_{marl}$ decreases to -16.37‰ at 537 cm BLF, only to increase to -15.46‰ at 531 cm BLF and remain at approximately that value for about 13.5 cm. $d^{18}O_{marl}$ makes a substantial increase to the highest value in the dataset, -13.59‰, at 505 cm BLF. The value decreases again to reach -15.00‰ at 503 cm BLF and experiences a gradual rise to -14.08‰ at 462.5 cm BLF and fall to -15.60‰ at 423 cm BLF over 80 cm. $d^{18}O_{marl}$ increases to reach -14.23‰ at 404 cm BLF, and decreases to -16.64‰ at 388 cm BLF. The $d^{18}O_{marl}$ values increase again to -14.83‰ at 381 cm BLF and remain at roughly that value until decreasing to -16.41‰ at 360 cm BLF. They remain between -17.20‰ and -16.61‰ until increasing again to -14.79‰. They remain at roughly this value for 13 cm until decreasing to -17.39‰ at 316 cm BLF and remain there until the end of the marl deposits at 276.5 cm BLF.

5.9 Carbon isotopes

The $d^{13}C_{marl}$ values from the 51 samples yielding sufficient $CaCO_3$ have a wider range of variability (8.69‰ between 604 and 276.5 cm BLF) than the $d^{18}O_{marl}$ values from the same samples (Fig. 13). The lowest $d^{13}C_{marl}$ value reached -10.82‰ at 350 cm BLF, while the highest value reached -2.13‰ at 505 cm BLF. The first $d^{13}C_{marl}$ value in the dataset is -4.08‰ at 604 cm BLF. The $d^{13}C_{marl}$ values exhibit a series of fluctuations between 604 and 562 cm BLF.

Here, the $d^{13}C_{marl}$ values decrease and recover twice by an average of about 2.50‰ (the lowest values averaging about -7.77‰ and the highest values averaging about -5.10‰). They decrease again to reach -7.99‰ at 537 cm BLF, and increase initially to a value of -4.65‰ at 531 cm BLF. They remain here until increasing again to the highest $d^{13}C_{marl}$ value in the dataset of -2.13‰ at 505 cm BLF. The value decreases to -3.95‰ at 503 cm BLF and increases again to reach -2.32‰ at 484 cm BLF. Values decrease steadily for 61 cm until reaching -8.94‰ at 423 cm BLF. Values increase to reach -5.79‰ at 404 cm BLF, then decrease again reaching -8.26‰ at 395.5 cm BLF.

6. INTERPRETATION

6.1 Interpretation of core stratigraphy

Basal deposits of glacial clay and silt (unit 1; Fig. 6) are consistent with the final glacial retreat from the Kenai Lowland ~15 ka and suggest rapid melting of the kettle-forming ice block. Clay deposits may also be indicative of meltwater deposits prior to hillslope stabilization by vegetation during retreat from the Skilak stade (~17.5 - 16.0 ka) and/or the Elmendorf Stade (~15.0 - 11.0 ka).

Gray to yellow marl laminated with organic-rich mud (unit 2; Fig. 6) deposited between ~14.0 and ~12.0 ka implies that the lake level at the core site was shallow enough (1-3 m) to support marl production from *Chara*. A thick (~2.5 cm) layer of peat deposited at ~12 ka likely represents basin desiccation and shoreline conditions promoting peat formation. Following this, about 7 cm of laminated marl and organic material implies that the lake level rose and the core site shifted back to shallow water conditions, ideal for *Chara* growth.

A sharp contact between laminated marl and organic material and medium-gray marl with lower $CaCO_3$ content (unit 3; Fig. 6) at ~11.9 cal kyr BP likely represents environmental conditions not ideal for *Chara* growth and marl production. The basin may have shallowed due to drier and potentially cooler conditions resulting in a shift in the zone of marl production and/or a decrease in *Chara* productivity. Alternatively, an increase in precipitation may have caused an influx of light attenuating particles such as recently deposited glacial clay and

silt resulting in poor conditions for charophyte growth. This unit lasts until ~11.4 cal kyr BP, suggesting that lake level remained stable during this time.

A shift back to marl deposits with higher $CaCO_3$ content at ~11.4 cal kyr BP (unit 4; Fig.6) implies that the lake experienced warmer conditions promoting *Chara* growth and/or a change in lake levels and a shift in the zone of marl production back to the core site. Between ~11.4 and ~8.8 cal kyr BP the stratigraphy suggests the lake experienced multiple deepening and shallowing events shifting the zone of marl production. Between ~10.8 and ~10.5 cal kyr BP the stratigraphy shifts to light brown marl indicating deeper water conditions with less *Chara* growth and marl deposition. Following this, the marl deposits become lighter suggesting lake level fall and a shift in the zone of marl production. Within this unit lies a 3 cm layer of pure, light yellow marl deposited at ~10.2 cal kyr BP. The occurrence of this "pure" marl suggests a interval of high productivity due to ideal environmental conditions for *Chara* growth (e.g. shallow water, 1-3 m deep, and a warm climate favorable to charophyte growth). Between ~10.0 and ~9.6 cal kyr BP the stratigraphy shifts back to light brown marl indicating a rise in lake level. The deposits shift to lighter brown-yellow marl suggesting drier conditions resulting in lake level fall.

At ~9.0 cal kyr BP the stratigraphy makes a gradual transition to more organic-rich mud with low $CaCO_3$ interbedded with four thick (~2 cm) layers of peat, three of which are overlain by 1-3 cm-thick marl deposits (unit 5; Fig. 6). The first peat layer (346 cm BLF) is likely not *in situ* as its character is not uniform and appears disturbed. Peat forms as either organic-rich deposits on the

lake floor in deep water conditions, or as fibrous peat on the shorelines and in very shallow water of lakes and ponds. Shoreline-formed peat is often accompanied by marl deposits in the sediment record of carbonate lakes (Wisconsin Dept. of Transportation, 2017). Because it is unlikely that lake levels would rise to deep enough depths to deposit deep-water peat at the core site, and that these peat deposits are associated with marl deposits, these peat layers were likely formed in shoreline conditions. This stratigraphy can be interpreted multiple ways which suggest various lake level responses to environmental change: (1) The lake may have experienced stepwise lake level rise with periods of lake level stability. In this scenario, peat deposits would develop at the lake shoreline through seasonal plant growth and die-back during periods of stable lake level. A rise in lake level would shift both the peat and marl production zones depositing a layer of marl on top of the recently deposited peat. Lake level remains stable again allowing for marl deposits to build thus shallowing the water depth and shifting the zone of peat formation back to the core site and starting the succession again. (2) Alternatively, this stratigraphic succession may represent frequent and significant lake level fluctuations where the peat layers represent periods of lake level lowering and shoreline conditions promoting peat deposition, and the intercalated marl units are interpreted as shallow-water conditions. In this scenario, immediately following shoreline peat deposition during lake level fall, the water depth at the core site likely rose at least to 1 m to promote *Chara* growth and carbonate precipitation.

A major shift in stratigraphy from dominant marl deposits with intermittent peat layers to loose, organic-rich mud with no $CaCO_3$ (unit 6) occurs at ~7.1 kyr cal BP (284 cm BLF). At this time, lake level rose and assumed relatively modern conditions. As lake level rose, the zone of marl production shifted about 430 m east of the core site where shallow water promotes calcium carbonate growth.

6.2 Interpretation of carbonate precipitation

XRD analysis revealed the marl deposits to be composed of magnesium calcite, which is consistent with other studies conducted on *Chara*-precipitated marl lakes (Fig. 9; Diefendorf et al., 2007).

Furthermore, the presence of *Chara* oospores in the sediment record indicate that the calcium carbonate was precipitated primarily as a result of *Chara* photosynthetic processes. Because *Chara* growth is depth-dependent, the marl deposits are interpreted as indicative of low lake levels (e.g. 1-3 m water depth).

Myxophyceae is potentially the current precipitating agent of calcium carbonate in the shallow basin, as there was no evidence for *Chara* in the shallow basin at the time of core recovery in late June, 2018. Small green blooms of microalgae appeared directly over the underwater springs in the shallow basin (~0.5-0.75 m water depth). The surface core from ~0.75 m water depth exhibited green deposits in the top ~5 cm of sediment which is indicative of recently deposited myxophyceae blooms reported to settle on lake floors in sheltered sites, much like the shallow basin in Kelly Lake (Pentecost, 1978).

6.3 Total inorganic carbon (TIC)

The close tracking of TIC and $CaCO_3$ values in the analyzed samples may be indicative of increased rates of photosynthesis due to increased TIC availability. Greater availability of dissolved inorganic carbon (DIC) in the water column may result in higher rates of photosynthesis. Photosynthetic processes increase the pH directly surrounding the algae thus inducing precipitation and deposition of $CaCO_3$ (Murphy et al. 1980).

There was no significant correlation between $d^{18}O_{marl}$ and TIC (Fig. 11) implying that greater availability of DIC was not influenced by shifts in $d^{18}O$ of the lake water and thus not influenced by changes in precipitation source or evaporation. No significant correlation between $d^{13}C_{marl}$ and TIC (Fig. 11) implies that greater availability of DIC in the water column did not influence primary productivity in the lake.

6.4 Oxygen and carbon isotope interpretation

Close tracking of the isotope values occurs when evaporative conditions cause the lake level to fall. High correlation between the $d^{18}O$ and $d^{13}C$ values ($R \geq 0.70$) is indicative of a closed system (Talbot, 1990). Drier conditions increase ^{18}O due to preferential evaporation of ^{16}O. Evaporation subsequently concentrates nutrients allowing for a greater proportion of the lake floor to be occupied by the photic zone accelerating primary productivity and increasing $d^{13}C$ values.

A significant strong correlation ($p < 0.05$; $R = 0.83$; Fig. 12) between $d^{13}C_{marl}$ and $d^{18}O_{marl}$ suggests that between ~14.1 and ~6.9 cal ka BP, during the

time of marl deposition at the core site, Kelly Lake was likely a closed system (evaporation sensitive).

From the oxygen and carbon isotopic covariance during previously defined climate intervals such as the Bølling Allerød warm period (~12.9 - ~14 ka; $p < 0.05$; R = 0.85; Fig. 13), the YD cool interval (~11.7 - ~12.9 ka; $p < 0.05$; R = 0.82; Fig. 14), and the Early Holocene warm interval (~8.2 - ~11.7 ka; $p < 0.05$; R = 0.93; Fig. 15), we can infer that Kelly Lake was a closed system during each of these intervals. This isotopic record is thus interpreted as influenced by changes in P-E and precipitation water source.

6.5 Oxygen isotope interpretation

The estimated change in $d^{18}O_{Ca}$ per degrees Celsius of atmospheric temperature change is ~0.33‰ for mainland Alaska (Bailey et al., 2019). The observed range of $d^{18}O$ in this dataset is 3.99‰ which corresponds to a temperature range of ~12.0 degrees Celsius. This wide temperature range is unlikely to occur over a span of ~7.2 ka. Although changes in temperature may have some effect on changes in $d^{18}O$, it is likely not the sole driver.

A large seasonal difference in $d^{18}O$ values exist between the winter and summer months in the Kenai lowland. Using Bowen's online water isotope calculator, annual precipitation $d^{18}O$ averages to -15.9‰, with winter precipitation closer to -19‰ and summer precipitation closer to -13‰ (Bowen, 2018). Current $d^{18}O$ isotopic composition of the Kelly Lake water is close to meteoric water composition (-14‰ to -13‰; Ellie Broadman pers. com.),

implying that there is currently little evaporative influence on the isotopic composition of the lake water.

Southwesterly storms are more frequent during periods of strengthened AL and provide more precipitation to the Kenai Peninsula than northeasterly storms. Although southwest precipitation is often enriched in ^{18}O, because Kelly Lake is likely a closed system for the duration of its marl record, the isotopic composition will be greater influenced by evaporative ^{18}O enrichment rather than meteoric ^{18}O enrichment. Furthermore, the low $d^{18}O$ values in this record have been further depleted through kinetic effects of *Chara* precipitation and are therefore not low enough to be sourced from isotopically lighter precipitation from the northeast.

The $d^{18}O_{marl}$ record begins with a value of -14.43‰ at ~14.1 cal kyr BP (Fig. 9). The values decrease slightly only to increase again to -14.56‰ at ~13.0 cal kyr BP, corresponding with the Bølling Allerød warm period and the isotope record on the Kenai Peninsula reported by Jones et al. (2014). Values decrease sharply to reach a low value of -16.06‰ at ~12.7 cal yr BP, corresponding with the onset of the YD and supporting cold and dry conditions not conducive to evaporation. Values increase slightly in the middle of the YD (-15.46‰; ~12.4 cal kyr BP) and remain there until reaching a sharp increase to -13.59‰ towards the end of the YD (11.9 cal kyr BP), suggesting warmer, evaporative conditions, or a shift to a more southwesterly moisture source bringing isotopically heavier precipitation. $d^{18}O_{marl}$ values increase gradually to reach -14.08‰ at ~11.2 cal kyr BP, roughly at the onset of the HTM in southcentral Alaska. There is a slight overall decrease in $d^{18}O_{marl}$ values during the Early Holocene until they increase

again at ~10.4 cal kyr BP (-14.70‰) and peak at ~10.0 cal kyr BP (-14.23‰) coinciding with the climatic high during the HTM and suggesting warm, dry conditions and high rates of evaporation. Values decline until they reach -17.20‰ at ~8.8 cal kyr BP, potentially suggesting cooler and wetter conditions following the HTM. The $d^{18}O_{marl}$ values then exhibit a sharp increase followed by a ~600-year interval (~9.6 - ~9.0 cal kyr BP) of higher values ranging between -14.83‰ and -14.92‰ suggesting warmer and drier conditions. The values then decrease abruptly and experience a ~600-year interval (~9.0 - ~8.6 cal kyr BP) of low $d^{18}O_{marl}$ ranging from -16.41‰ to -17.20‰ suggesting cooler and wetter conditions and freshening of the water column with isotopically lighter precipitation. Following this, they experience a shift back to either evaporative conditions or to dominant summer precipitation and southerly moisture sources evidenced by a sharp increase followed by another ~500-year interval (~8.6 - ~8.1 cal kyr BP) of higher values ranging from -14.77‰ and -14.97‰. Another shift to cool and wet conditions or greater winter precipitation and northerly storm tracks is evidenced by a sharp decrease to -17.39‰ at ~8.0 cal kyr BP. The values remain there until the end of the marl deposits at ~6.9 cal kyr BP.

6.6 Carbon isotope interpretation

Shifts in $d^{13}C$ values likely reflect changes in the composition of dissolved inorganic carbon (DIC) in the water column. In the Kelly Lake record, elevated $d^{13}C$ values likely result from increased primary productivity in the water column during closed basin conditions and lower lake level. More negative $d^{13}C$ values may be indicative of an increase in groundwater input which is typically

isotopically lighter (-10‰ to -15‰). Due to the presence of underwater springs in Kelly Lake, periods of increased effective moisture causing increased groundwater input are likely reflected in the isotopic record as more negative $d^{13}C$ values. Furthermore, physical dynamics between the groundwater input and lake level may be involved where lower lake level draws more groundwater in to the lake raising the lake level and depleting the water column in ^{13}C. A strong covariance between the oxygen and carbon isotopes implies that there is a strong evaporative influence on the isotopic signals. With greater rates of evaporation, lake level falls and the photic zone occupies a higher percentage of the lake floor. This increases primary productivity and depletes ^{12}C in the water column. In the record presented here, the carbon isotopic signal is interpreted as reflective of lake level change due to shifts in P-E.

The $d^{13}C_{marl}$ values follow a similar trend to the oxygen isotope values. They begin high, reaching -4.08‰ at ~14.1 cal kyr BP, suggesting potentially higher rates of primary productivity at the onset of the Bølling Allerød (Fig. 9). The values then exhibit a series of fluctuations throughout the Bølling Allerød, suggesting either drastic and rapid shifts in primary productivity or shifts in precipitation rates increasing groundwater input and depleting the signal. A drop in $d^{13}C_{marl}$ values to -7.99‰ at ~12.6 cal kyr BP coincide with the onset of the YD, supporting colder and drier conditions less conducive to lake productivity. The values experience a rapid increase initially at ~12.4 cal kyr BP reaching -4.65‰ suggesting a major shift in primary productivity. $d^{13}C_{marl}$ values reach a peak of -2.13‰ at ~11.9 cal kyr BP, suggesting enhanced primary productivity in

the latter half of the YD. Values decline slightly only to increase to -2.32‰ at ~11.6 cal kyr BP at the beginning of the Early Holocene, suggesting warm and dry conditions at its onset. A steady and significant decline in $d^{13}C_{marl}$ values at the onset of the HTM until reaching a low value of -8.94‰ at ~10.5 cal kyr BP imply that Kelly Lake responded strongly to regional environmental shifts. Values peak again shortly after at ~10.4 cal kyr BP (-6.39‰) and remain high until ~10.1 cal kyr BP (-5.79‰) at the peak of the HTM supporting warm and dry conditions as purported in Kaufman et al., 2010. Values decline again to -10.21‰ at 9.8 cal kyr BP, suggesting a shift in productivity in the lake in response to cooler conditions and/or lake level rise. $d^{13}C_{marl}$ values then experience several intervals of high and low isotopic values closely corresponding to shifts in the $d^{18}O$ record. A ~600-year interval (~9.6 to ~9.0 cal kyr BP) of elevated $d^{13}C$ values (-7.5‰ to -5.92‰) suggest low lake levels and evaporative conditions with high productivity. Following this, a ~600-year interval (~9.0 to ~8.6 cal kyr BP) of low $d^{13}C$ values (-9.24‰ to -10.82‰) indicate wetter conditions and/or lower lake level inducing groundwater input and promoting lake level rise. Another ~500-year interval (~8.6 to ~8.1 cal kyr BP) of higher $d^{13}C$ values (-5.89‰ to -5.33‰) immediately follows suggesting a rapid shift drier conditions promoting lower lake levels and higher rates of productivity. The values decrease rapidly again to reach -9.03‰ at ~8.0 cal kyr BP and continue to decline gradually for the remainder of the marl record until reaching -10.55‰ at ~6.9 cal kyr BP suggesting a shift to wetter conditions and/or an increase in groundwater input and higher lake level.

7. DISCUSSION

Presented here are multiple interpretations of Kelly Lake's response to environmental change on the Kenai Peninsula based on four proxies: $d^{18}O$ and $d^{13}C$ values, stratigraphic interpretation, and $CaCO_3$ content. Although the data presented here strongly suggests that Kelly Lake was a closed basin and evaporation sensitive during the period of marl deposition (~14.1-6.9 cal kyr BP), there is strong evidence in the literature for AL and moisture source influence on precipitation rate and isotopic compositions in paleoenvironmental records. This record is therefore interpreted as influenced by both changes in P-E and precipitation source water influencing precipitation rate.

7.1 Paleoenvironmental interpretation

Bølling Allerød

The peak $d^{18}O_{marl}$ value (14.56‰) within the Bølling Allerød as defined by the age model coincides with the peak of the Bølling Allerød warm period at ~13.0 cal kyr BP (Fig. 6). Higher $d^{18}O_{marl}$ values during this time are likely influenced by a warmer climate, evaporative conditions, and lower lake level. Lake level was likely lower and the basin was closed due to recent lake formation following glacial retreat. This is supported by high rates in primary productivity evidenced by elevated $d^{13}C$ and $CaCO_3$ values.

Younger Dryas

During the YD, the lake is interpreted as a closed basin based on the strong covariance between the $d^{18}O_{marl}$ and $d^{13}C_{marl}$ values. This implies that the

lake had a strong evaporative influence at this time. However, because the YD is defined by presumably cooler temperatures, this would result in a weaker evaporative influence and a stronger influence from shifts in moisture source and temperature changes. Multiple interpretations of the data from the YD are therefore described.

Higher calcite precipitation rates at the core site towards the beginning of the YD, evidenced by high values of $CaCO_3$ and light gray to yellow marl deposits with faint organic mud laminations, imply that the lake experienced higher rates of *Chara* productivity at this time. This contrasts with previous studies on the Kenai suggesting that lakes experienced lower rates of primary productivity due to lake level fall and lower temperatures (Kaufman et al., 2010). However, decrease in effective moisture at the onset of the YD may have reduced light attenuating particle transport to the lake, thus promoting charophyte growth in shallow waters.

This interpretation is not supported by the isotopic record presented here which suggests greater precipitation and groundwater input at the start of the YD. This caveat is reconciled with the fact that colder conditions at the onset of the YD are well supported in the literature. Colder conditions would complicate the isotopic interpretation presented here and the low $d^{18}O$ values at the YD onset may be indicative of cold conditions not conducive to evaporation and reduced effective moisture promoting clear and shallow water conditions ideal for charophyte growth.

Based on our age model, at around 12.0 to 12.1 cal kyr BP lies a 2 cm deposit of peat overlain by a 7 cm of laminated marl and organic matter accompanied by an abrupt increase in $d^{18}O_{marl}$. This suggests rapid desiccation of the basin and deposition of shoreline peat due to increased temperatures and decreased effective moisture promoting evaporation. The overlying marl unit with a high $d^{18}O$ value suggests a rise in lake level and a return to shallow lake conditions promoting charophyte growth at the core site. This increase in effective moisture and lake level rise is supported by the replacement of a wetland with an oligotrophic lake at Discovery Pond about 12.2 ka as reported by Kaufman et al. (2004).

Elevated $d^{13}C_{marl}$ and $d^{18}O_{marl}$ values accompanied by a sharp shift in sediment character from laminated marl and organic material to gray marl with low $CaCO_3$ content between ~11.9 cal kyr BP and ~11.4 cal kyr BP can be interpreted a couple different ways: (1) If the lake had a strong evaporative influence at this time, this shift to less negative $d^{18}O$ values would be indicative of evaporative conditions resulting in increased productivity in the lake causing ^{13}C enrichment in the water column. It is difficult to reconcile this interpretation in the stratigraphy which shows a sharp shift to gray marl with low $CaCO_3$ content implying that conditions were not ideal for charophyte growth which would presumably decrease primary productivity in the lake. While charophytes may not have thrived in this environment at the time, the increase in temperature after a cold period may have supported an increase in productivity of other aquatic plants in the lake, thus complicating *Chara* growth and marl production. Drier

conditions would also decrease groundwater input to the lake thus depleting the bicarbonate supply needed for *Chara* photosynthesis. This interpretation is not consistent with other studies suggesting a shift to wetter conditions towards the end of the YD (~12.2 ka; Kaufman et al., 2010). (2) If the isotopic composition of meteoric water influenced the composition of the water column, the $d^{18}O$ values may suggest a shift to more southwesterly storms providing warmer air and greater precipitation to the lake. These results would therefore support wetter and warmer conditions at the close of the YD but are expressed about 800 years later (~11.4 cal kyr BP), suggesting a later onset of these wetter conditions than previously thought. Alternatively, this age disparity could be a product of inaccuracy in our age model. More ^{14}C dates are needed to better constrain this model.

Early Holocene

Following the gray marl unit, the stratigraphy shifts back to marl with higher $CaCO_3$ content at ~11.2 cal kyr BP suggesting a shift to lake conditions ideal for charophyte growth at the onset of the Holocene. Also at this time, $d^{13}C_{marl}$ and $d^{18}O_{marl}$ values become more positive suggesting continued low lake levels. At ~11.1 cal kyr BP both $d^{18}O$ and $d^{13}C$ values begin to gradually decline. This shift is accompanied by a gradual transition to medium- to light-brown marl with lower $CaCO_3$ values. This is interpreted as a rise in lake level resulting in the zone of marl production to shift out of the core site. The lake is interpreted as a closed system at this time and thus this isotopic record suggests that the lake experienced a freshening of the water column due to increased effective moisture

(presumably due to a strengthened AL and a shift to more southwesterly precipitation) and an increase in isotopically depleted groundwater. At about ~10 cal kyr BP, deposition of pure, yellow marl accompanied by a spike in $d^{18}O_{marl}$ and $d^{13}C_{marl}$ values coincide with the warm conditions of the Holocene Thermal Maximum (HTM). The rise in $d^{18}O_{marl}$ values suggest high rates of evaporation due to the warm temperatures, resulting in low lake levels (1-3 m at the core site) and enhanced primary productivity as evidenced by the high $d^{13}C_{marl}$ values. This interpretation of warm and dry conditions is supported in the literature by Kaufman et al. (2010) and Anderson et al. (2006).

Variable conditions and multiple lake level fluctuations are observed in the latter part of the Early Holocene (~10.0 - 7.4 cal kyr BP). Following the warm and dry conditions of the HTM promoting low lake level and marl deposition, $d^{18}O$ and $d^{13}C$ values decline along with a shift to medium- to light-brown marl mud with lower $CaCO_3$ values indicating an increase in effective moisture resulting in lake level rise between ~9.9 and 9.7 cal kyr BP. This decline in primary productivity and lake level rise is supported in other records such as the BSi record from Arolik Lake (Hu et al., 2006). Lake level fall is apparent in the stratigraphic shift to lighter brown marl mud with higher $CaCO_3$ content accompanied by higher $d^{18}O$ and $d^{13}C$ values between ~9.6 and 9.1 cal kyr BP. This suggests more evaporative conditions and a decrease in effective moisture potentially caused by a weakening of the AL. At ~9.0 cal kyr BP the stratigraphy makes a gradual transition to more organic-rich mud containing less $CaCO_3$. This likely represents lake level rise due to increased effective moisture and

groundwater input. This shift is supported by a decrease in BSi% around this time in both Arolik Lake (Hu et al., 2006) and Discovery Pond (Kaufman et al., 2010). These more negative isotope values in the Kelly Lake record are also accompanied by a layer of peat in the stratigraphic record (Fig. 6). This layer does not, however, appear *in situ* suggesting that is does not represent basin desiccation and shoreline conditions. Drier conditions likely followed this period as supported by a major shift to higher $d^{18}O$ and $d^{13}C$ values between ~8.5 and 8.1 cal kyr BP. This climatic shift is also supported in the stratigraphic record by deposition of presumably shoreline peat following this period of high isotopic values indicating evaporative conditions and basin desiccation. The stratigraphy here shows a decrease in marl production which had been interpreted previously in this record as indicative of lake level rise and marl production zone shift. However, with the arrival of *P. glauca* (white spruce) around 8.5 ka (Anderson et al., 2006) it is likely that the lake experienced an increase in humic acid input effectively inhibiting charophyte production. Following this period of basin desiccation and peat deposition, a layer of marl is accompanied by a shift to more negative isotope values at ~8.0 cal kyr BP. This suggests an increase in effective moisture, freshening of the water column, and lake level rise. This marl unit and the two above it differs slightly in character from the majority of the marl deposits in this record. Their color is more greenish and it appears more mottled. This may indicate a shift in the primary precipitating agent in the lake from charophytes to myxophyceae. Following the ~8.0 cal kyr BP rise in lake level, the isotopic values remain low indicating continual wet conditions and freshening of the water

column. The stratigraphic sequence here suggests stepwise lake level rise due to increased effective moisture with periods of lake level stability.

However, if northerly storm tracks provided most of the precipitation to the peninsula, the isotopic signature would likely become more negative where a dominant southern precipitation source would enrich the isotopic values in the record. The limitation to this interpretation lies in the isotopic disequilibrium between the water column and *Chara*-precipitated marl. Due to this disequilibrium, the lower $d^{18}O_{marl}$ values may actually reflect meteoric water compositions closer to 14.0‰ which indicate a more southerly moisture source. This limitation results in a stronger preference for the first interpretation suggesting a strong P-E signal and subsequent stepwise lake level rise.

This cyclical pattern in the isotope values of the Early Holocene may also be a result of feedback mechanisms involving lake level and groundwater input. For example, when lake level was higher, groundwater input from the underwater springs may decrease due to increase pressure in the water column. This may result in eventual fall in lake level causing the pressure in the water column to decrease thus increasing groundwater input and subsequently raising lake level.

The marl record ends at ~6.9 cal kyr BP. Although there are no isotopic signals reported for ~6.9 cal kyr BP to present in this record, based on the visual stratigraphy, lake level likely assumed relatively modern conditions and lake level at ~7.4 cal kyr BP (Fig. 6). This is consistent with Anderson et al. (2005) who conducted analysis on a groundwater-fed lake in Yukon Territory. Their core stratigraphy suggests that the physical and chemical characteristics of the modern

lake have been stable for the last ~7.5 ka. This shift to consistently higher lake levels and an apparent freshening of the water column as evidenced by the isotopic record may have resulted from a shift to a predominantly southwestern moisture source increasing effective moisture. This theory is also supported by the increase in tephra abundance at the same time (Fig. 6). Storms and winds tracking from the southwest would presumably bring more ashfall from the Aleutian Arc depositing tephra layers in Kelly Lake.

8. CONCLUSION

The relationship between isotopic values in *Chara*-precipitated marl deposits and the isotopic signal of a closed basin which is also likely influenced by the shifting strength and position of the AL is difficult to untangle. The AL likely had some influence on isotopic values presented here, but based on the overall correlation between $d^{18}O_{marl}$ and $d^{13}C_{marl}$ for the entire dataset, plus stratigraphic evidence for lower lake level than present, the lake is assumed to have maintained a closed basin and long residence times during the period of marl deposition at the core site. Our data reported here both support and contradict many previous studies of climate change on the Kenai Peninsula. The Kelly Lake record suggests fluctuating environmental conditions in the lake during the Bølling Allerød and lake formation and stabilization. High isotopic values at the close of the Bølling Allerød support warm and dry conditions. This record supports cool and dry conditions at the onset of the YD, with climatic conditions promoting clear waters and charophyte growth. Basin desiccation and shoreline setting at the core site due to dry conditions at around 12.0 to 12.1 cal kyr BP are supported here. An increase in effective moisture at around 12.2 cal kyr BP as purported by Kaufman et al. (2004) is also supported by the Kelly Lake record. The lake likely experienced a shift in lake level, chemistry, clarity, and ecological state between ~11.9 and 11.4 cal kyr BP. This portion of the record is difficult to interpret and further investigation in to the age model and percentage of terrigenous material is warranted. The lake experienced multiple water level fluctuations during the Early Holocene due to shifting position of the AL and

precipitation rate and/or physical dynamics between lake level and groundwater input. These fluctuations are supported in the records from Hu et al. (2006) and Kaufman et al. (2010). This record also supports warm and dry conditions at the peak of the HTM. The lake assumed relatively modern conditions at ~6.9 cal kyr BP presumably due to a shift to a moisture source from the southwest providing greater effective moisture as well as ashfall from the Aleutian Arc. Furthermore, this study contributes to the ongoing research on the reliability of marl deposits precipitated from *Chara* as indicators of climatic change.

References

Abbott, M.B., Finney, B.P., Edwards, M.E., Kelts, K.R., 2000. Lake-level reconstruction and paleohydrology of Birch Lake, central Alaska, based on seismic reflection profiles and core transects. Quat. Res. 53, 154e216.

Anderson, L., Abbott, M.B., Finney, B.P., Burns, S.J. 2005. Regional atmospheric circulation change in the North Pacific during the Holocene inferred from lacustrine carbonate oxygen isotopes, Yukon Territory, Canada. Quaternary Research 66 (2005) 21-25. doi:10.1016/j.yqres.2005.03.005

Anderson, R.S., Hallett, D.J., Berg, E., Jass, R.B., Toney, J.L., de Fontaine, C.S., DeVolder, A., 2006. Holocene development of boreal forests and fire regimes on the Kenai Lowlands of Alaska. The Holocene 16, 791e803.

Anderson, L., Abbott, M.B., Finney, B.P., Burns, S.J., 2007. Late Holocene moisture balance variability in the southwest Yukon Territory, Canada. Quat. Sci. Rev. 26, 130e141. http://dx.doi.org/10.1016/j.quascirev.2006.04.011.

Andrews J., Coletta P., Pentecost A., Riding R., Dennis S., Dennis P.F., Spiro B. 2004. Equilibrium and disequilibrium stable isotope effects in modern charophyte calcites: implications for palaeoenvironmental studies. Palaeogeography, Palaeoclimatology, Palaeoecology 204: 101-114.

Apolinarska, K., Pełechaty, M., Pukacz, A. 2011. CaCO3 sedimentation by modern charophytes (Characeae): can calcified remains and carbonate δ13C and δ18O record the ecological state of lakes? – a review. Studia Limnologica et Telmatologica 5, 2, 55-66

Barron, J.A., Bukry, D., Dean, W.E., Addison, J.A., Finney, B., 2009. Paleoceanography of the Gulf of Alaska during the past 15,000 years: Results from diatoms, silicoflagellates, and geochemistry. Marine Micropaleontology 72, 176e195.

Bathurst, R.G.C. 1975. Recent carbonate algal stromatolites. In: Bathrust, C.G.C. (ed.), Carbonate sediments and their diagenesis, Series Developments in Sedimentology 12, 217–230. Elsevier, Amsterdam.

Berg, E.E. 2018. Lateglacial and Holocene lake level fluctuations on the Kenai Lowland, based on satellite-fen peat deposits and ice-shoved ramparts, Kenai Peninsula, AK (UNPUBLISHED)

Clark, S.H.B. 1973. The McHugh Complex of South-Central Alaska. Contributions to Stratigraphy, Geological Survey Bulletin 1372-D

Coletta P., Pentecost A., Spiro B. 2001. Stable isotopes in charophyte incrustations: relationships with climate and water chemistry. Palaeogeography, Palaeoclimatology, Palaeoecology 173: 9-19.

Daigle and Kaufman. 2009. Holocene climate inferred from glacier extent, lake sediment and tree rings at Goat Lake, Kenai Mountains, Alaska, USA. Journal of Quaternary Science 24, 33-45

Diefendorf, A.F., Patterson, W.P., Holmden, C., Mullins, H.T. 2007. Carbon isotopes of marl and lake sediment organic matter reflect terrestrial landscape change during the late Glacial and early Holocene (16,800 to 5,540 cal yr B.P.): a multiproxy study of lacustrine sediments at Lough Inchiquin, western Ireland. Journal of Paleolimnology 39 (2008) 101-115

Field, R.D., Moore, G.W.K., Holdsworth, G., Schmidt, G.A., 2010. A GCM-based analysis of circulation controls on d18O in the southwest Yukon, Canada: implications for climate reconstructions in the region. Geophys. Res. Lett. 37, L05706. http://dx.doi.org/10.1029/2009GL041408.

de Fontaine, C.S., Kaufman, D.S., Anderson, R.S., Werner, C., Waythomas, C.F., Brown, T.A. 2007. Late Quaternary distal tephra-fall deposits in lacustrine sediments, Kenai Peninsula, Alaska. Quaternary Research 68 (2007) 64-78

Hu, F.S., Nelson, D.M., Clarke, G.H., Rühland, K.M., Huang, Y., Kaufman, D.S., Smol, J.P., 2006. Abrupt climatic events during the last glacial-interglacial transition in Alaska. Geophysical Research Letters 33, L18708.

Jones, M.C., Peteet, D.M., Kurdyla, D., Guilderson, T., 2009. Climate and vegetation history from a 14,000-year peatland record, Kenai Peninsula, Alaska. Quat. Res. 72, 207e217. http://dx.doi.org/10.1016/j.yqres.2009.04.002.

Jones, M.C., Wooller, M., Peteet, D.M. 2014. A deglacial and Holocene record of climate variability in south-central Alaska from stable oxygen isotopes and plant macrofossils in peat. Quaternary Science Reviews 87 (2014) 1-11. doi:10.1016/j.quascirev.2013.12.025

Jones, M.C., Yu, Z., 2010. High sensitivity of Alaskan peatlands to temperature seasonality during the Holocene thermal maximum. Proc. Natl. Acad. Sci. U. S. A. 107, 7347e7352.

Kaufman, D.S., Anderson, R.S., Hu, F.S., Berg, E., Werner, A. 2010. Evidence for a variable and wet Younger Dryas in southern Alaska. Quaternary Science Reviews 29 (2010) 1445-1452

Kaufman, D.S., Axford, Y.L., Henderson, A.G.C., McKay, N.P., Oswald, W.W., Saenger, C., Anderson, R.S., Bailey, H.L., Clegg, B., Gajewski, K., Hu, F.S., Jones, M.C., Massa, C., Routson, C.C., Werner, A., Wooller, M.J., Yu, Z. 2016. Holocene climate changes in eastern Beringia (NW North America) -- A systematic review of multi-proxy evidence. Quaternary Science Reviews 147 (2016) 312-339

Kindle, E.M. 1927. The role of thermal stratification in lacustrine sedimentation. Trans. R. Soc. Canada, Ser. 3, No. 21, 1-36. In: Murphy, D.H., Wilkinson, B.H. 1980. Carbonate deposition and facies distribution in a central Michigan marl lake. Sedimentology 27, 123-135

Kindle, E.M. 1929. A comparative study of different types of thermal stratification in lakes and their
influence on the formation of marl. J. Geol. 37, 150-1 57. In: Murphy, D.H., Wilkinson, B.H. 1980. Carbonate deposition and facies distribution in a central Michigan marl lake. Sedimentology 27, 123-135

Kusky, T.M., Bradley, D.C. 1999. Kinematic analysis of mélange fabrics: examples and applications from the McHugh Complex, Kenai Peninsula, Alaska. Journal of Structural Geology 21. 117-1796

Leng, M.J., Marshall, J.D. 2004. Palaeoclimate interpretation of stable isotope data from lake sediment archives. Quaternary Science Reviews v23, issues 7-8, p 811-838

McKay, N.P., Kaufman, D.S., 2009. Holocene climate and glacier variability at Hallet and Greyling lakes, Chugach Range, south-central Alaska. Journal of Paleolimnology 41, 143e159.

Murphy, D.H., Wilkinson, B.H. 1980. Carbonate deposition and facies distribution in a central Michigan marl lake. Sedimentology 27, 123-135

Mantua, N.J., Hare, S.R., Zhang, Y., Wallace, J.M., Francis, R.C., 1997. A Pacific interdecadal climate oscillation with impacts on salmon production. Bulletin of the American Meteorological Society 78, 1069– 1079.

Moxham, R.M. and Eckhart, R.A. 1956. Marl deposits in the Knik Arm area, Alaska. Geological Survey Bulletin 1039 - A.

Pełechaty M., Apolinarska K., Pukacz A., Krupska J., Siepak M., Boszke P., Sinkowski M. 2010. Stable isotope composition of Chara rudis encrustation in a lake with extensive underwater charophyte meadows. Hydrobiologia 656: 29-42.

Pentecost, A., Blue-green algae and freshwater carbonate deposits. 1978. Proc. R. Soc. Lond. B 1978 200, doi: 10.1098/rspb.1978.0004

Pentecost A., Andrews J.E., Dennis P.F., Marca-Bell A., Dennis S. 2006. Charophyte growth in small temperate water bodies: Extreme isotopic disequilibrium and implications for the paleoecology of shallow marl lakes. Palaeogeography, Palaeoclimatology, Palaeoecology 240: 389-404.

Pettijohn, F. J., 1949, Sedimentary rocks: New York, Harper and Brothers. In: Moxham, R.M. and Eckhart, R.A. 1956. Marl deposits in the Knik Arm area, Alaksa. Geological Survey Bulletin 1039 - A.

Pronin, E., Pełechaty M., Apolinarska K., Pukacz A. 2018. Oxygen stable isotope composition of carbonate encrustations of two modern, widely distributed, morphologically different charophyte species. Hydrobiologia 809:41-52. https://doi.org/10.1007/s10750-017-3444-4

Pukacz, A., Pełechaty M., Frankowski, M. 2016. Depth-dependence and monthly variability of charophyte biomass production: consequences for the precipitation of

calcium carbonate in a shallow Chara-lake. Environ Sci Pollut Res (2016) 23:22433–22442. DOI 10.1007/s11356-016-7420-8

Reger, R.D., Sturmann, A.G., Berg, E.E., Burns, P.A.C., 2007. Guidebook 8. A Guide to the Late Quaternary History of the Northern and Western Kenai Peninsula, Alaska. State of Alaska Department of Natural Resources and Division of Geological and Geophysical Surveys, Alaska.

Reimer, P.J., Bard, E., Bayliss, A., Beck, J.W., Blackwell, P.G., Bronk Ramsey, C., Buck, C.E., Edwards, R.L., Friedrich, M., Grootes, P.M., Guilderson, T.P., Haflidason, H., Hajdas, I., Hatté, C., Heaton, T.J., Hoffmann, D.L., Hogg, A.G., Hughen, K.A., Kaiser, K.F., Kromer, B., Manning, S.W., Niu, M., Reimer, R.W., Richards, D.A., Scott, M.E., Southon, J.R., Turney, C.S.M., van der Plicht, J., 2013. IntCal13 and Marine13 radiocarbon age calibration curves 0-50,000 yr cal BP. Radiocarbon 55(4), 1869-1887 Riehle, J.R., Bowers, P.M., Ager, T.A., 1990. The Hayes tephra deposits, an upper Holocene marker horizon in south-central Alaska. Quaternary Research 33, 276–290. In: Blaauw, M., and Christen, J.A. Bacon Manual - v2.3.5.

Rip W.J., Ouboter M.R.L., Los H.J. 2007. Impact of climatic fluctuations on Characeae biomass in a shallow, restored lake in The Netherlands. Hydrobiologia 584: 415–424.

Sarnthein, M., Kiefer, T., Grootes, P.M., Elderfield, H., Erlenkeuser, H., 2006. Warmings in the far northwestern Pacific promoted pre-Clovis immigration to America during Heinrich event 1. Geology 34, 141e144.

Schiff, C.J., Kaufman, D.S., Wolfe, A.P., Dodd, J., Sharp, Z. 2008. Late Holocene storm-trajectory changes inferred from the oxygen isotope composition of lake diatoms, south Alaksa. J Paleolimnol 41:189–208 DOI 10.1007/s10933-008-9261-z

Talbot, M.R., 1990. A review of the palaeohydrological interpretation of carbon and oxygen isotopic ratios in primary lacustrine carbonates. Chemical Geology, Isotope Geosciences Section 80, 261–279

Trenbirth, K.E., Hurrell, J.W., 1994. Decadal atmosphere-ocean variations in the Pacific. Climate Dynamics 9, 303–319.

Welch P.S. 1935. Limnology: New York, McGraw-Hill Book Co.

Wetzel, R.G. 2001. Limnology: Lake and River Ecosystems, Third Edition. Elsevier Inc.

Winton, M.D., Dugdale, T.M., and Clayton, J.S. 2007. Identification of oospores of the extant charophytes of New Zealand. New Zealand Journal of Botany, 45:3, 463-476; DOI: 10.1080/00288250709509729

Wisconsin Dept. of Transportation. 2017. Geotechnical Manual, Ch 4: Organic Soils, Sect 2: Types and Descriptions

Yu, Z., Walker, K.N., Evenson, E.B., Hajdas, I., 2008. Lateglacial and early Holocene climate oscillations in the Matanuska Valley, south-central Alaska. Quaternary Science Reviews 27, 148e161.

Figures

A.

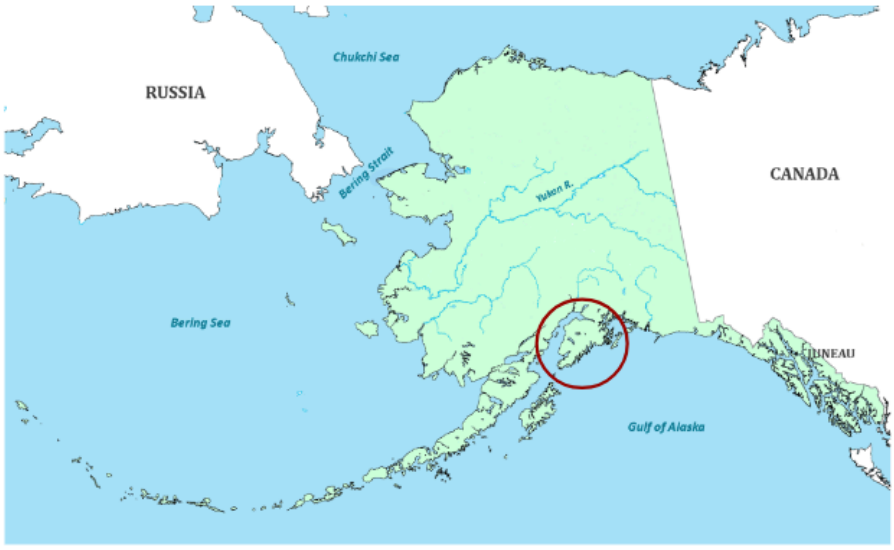

B.

Figure 1. (a) Map of Alaska with Kenai Peninsula circled in red. (b) Satellite image of Kenai Peninsula with Kelly Lake location defined by red pin.

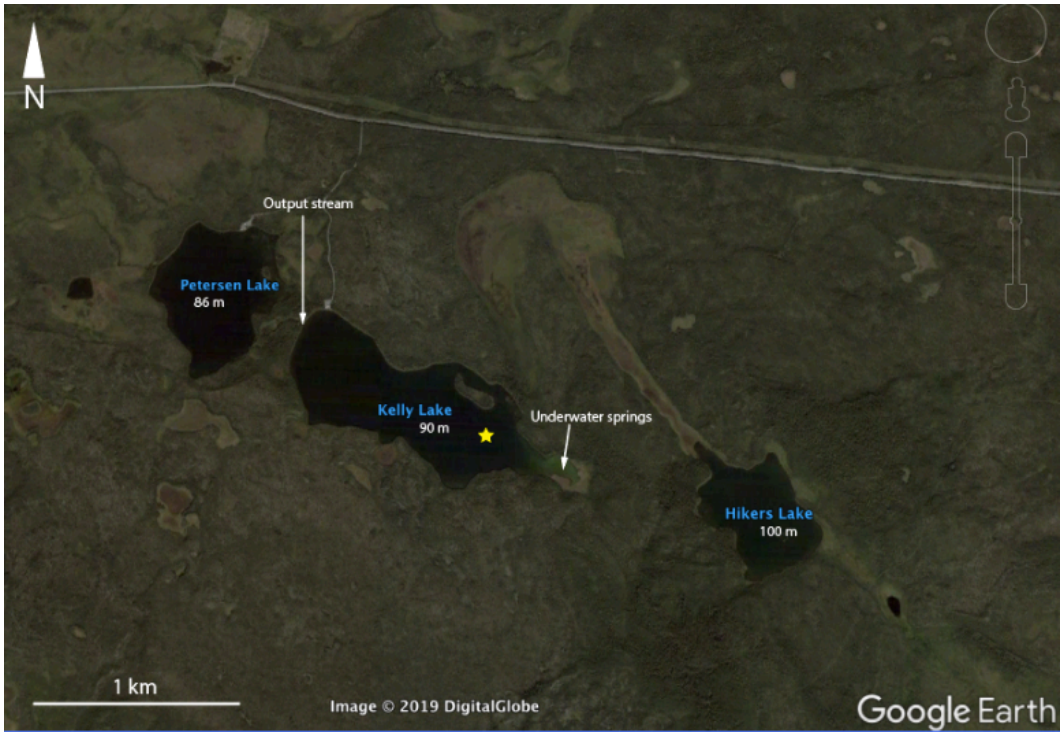

Figure 2. Satellite image of Kelly Lake showing shallow eastern bench and white lake bottom.

Figure 3. Photo of shoreline and bank vegetation taken from the lake. Dominant spruce with some birch and tall grasses are shown. Facing east. Kenai Mountains in the background.

Figure 4. Geotek MSCL-XYZ point sensor taking MS measurements every 0.5 cm.

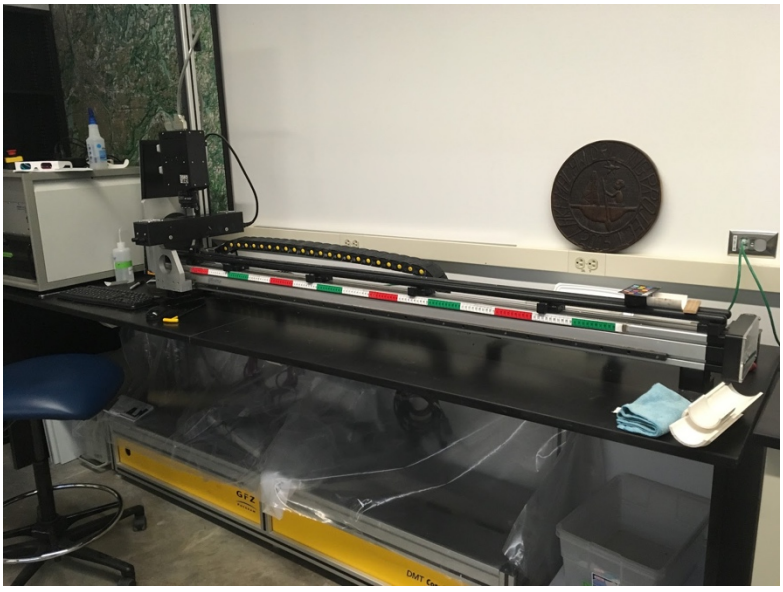

Figure 5. Geotek Geoscan-III camera.

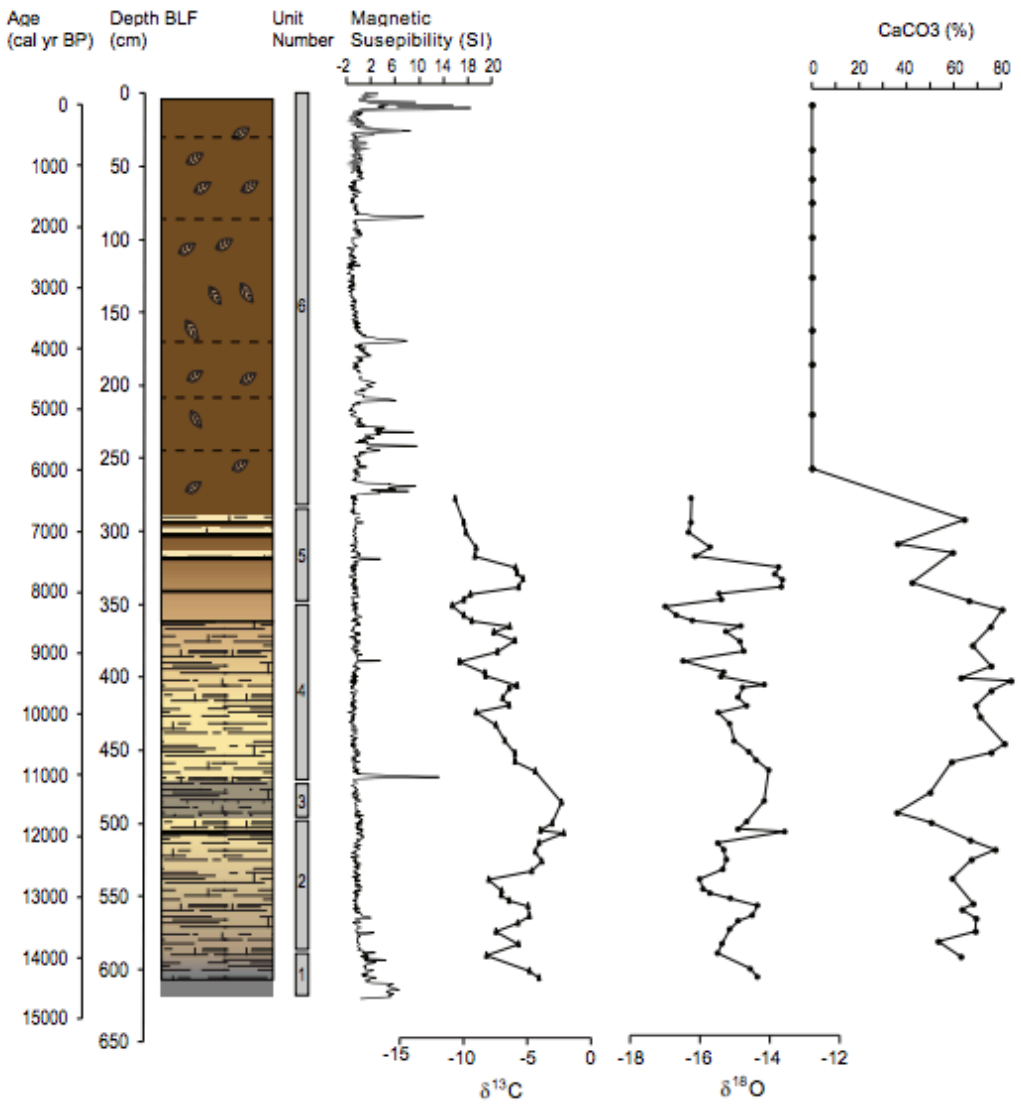

Figure 6. Stratigraphic column representing the defined units (1-6). Magnetic Susceptibility (SI), $d^{18}O$ isotopes, $d^{13}C$ isotopes, and $CaCO_3$ plotted at the core depth represented in the stratigraphic column.

Figure 7. *Chara* oospore among dried marl deposit. Width of oospore ~0.5mm

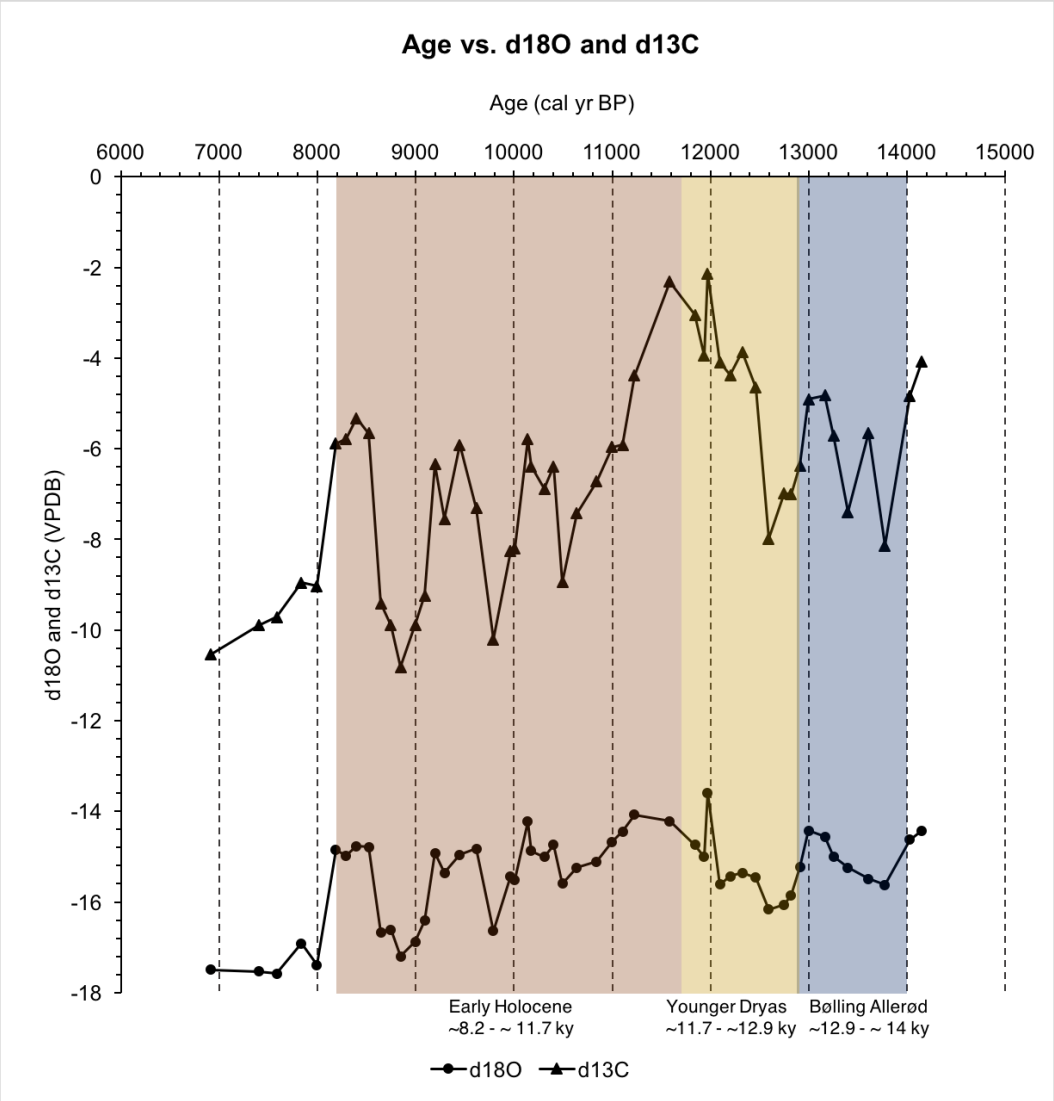

Figure 8. Age (cal BP) versus $d^{18}O$ and $d^{13}C$ (‰) values analyzed for 51 samples from KLY18-4. Based on the age model, the ages of the samples ranged from 14152 cal yr BP, the beginning of the Bølling Allerød warm period (~14 ka), to 6910 cal yr BP, about 800 years after the ending of the climate interval defined as the Early Holocene (~8.2 ka).

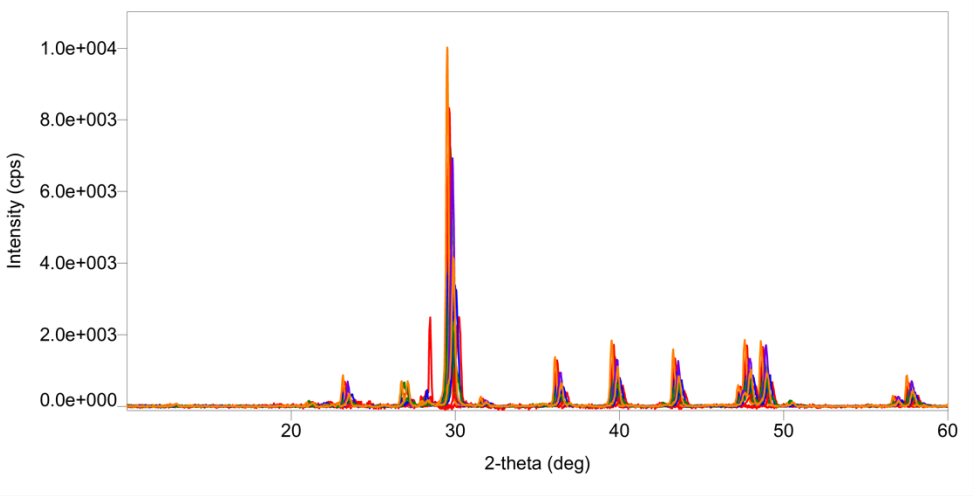

Figure 9. Graph showing XRD output. Multiple colored lines indicate different samples tested. Signals from all samples indicate calcium carbonate.

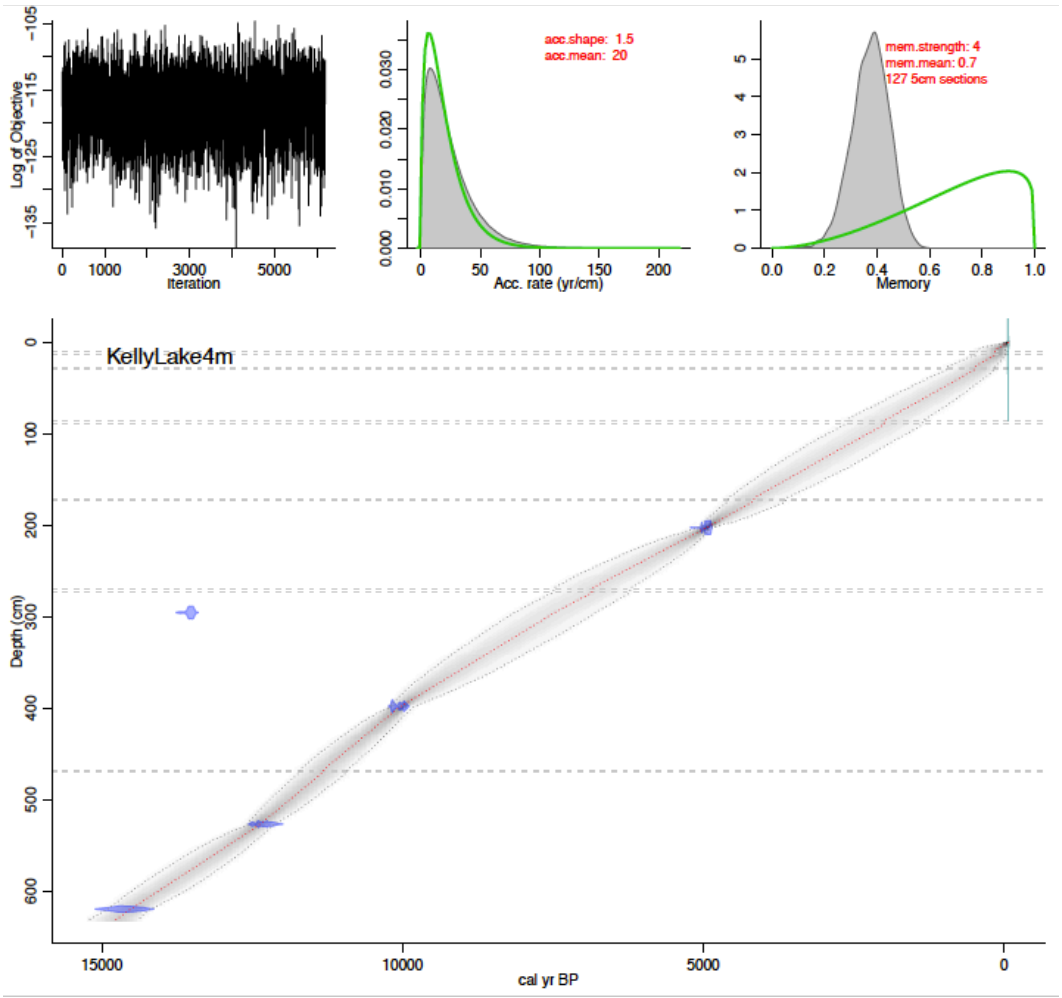

Figure 10. Age model output from Bacon. Blue ovals represent calibrated ^{14}C dates throughout the core. Grey shading indicates standard deviation for ages between calibrated dates.

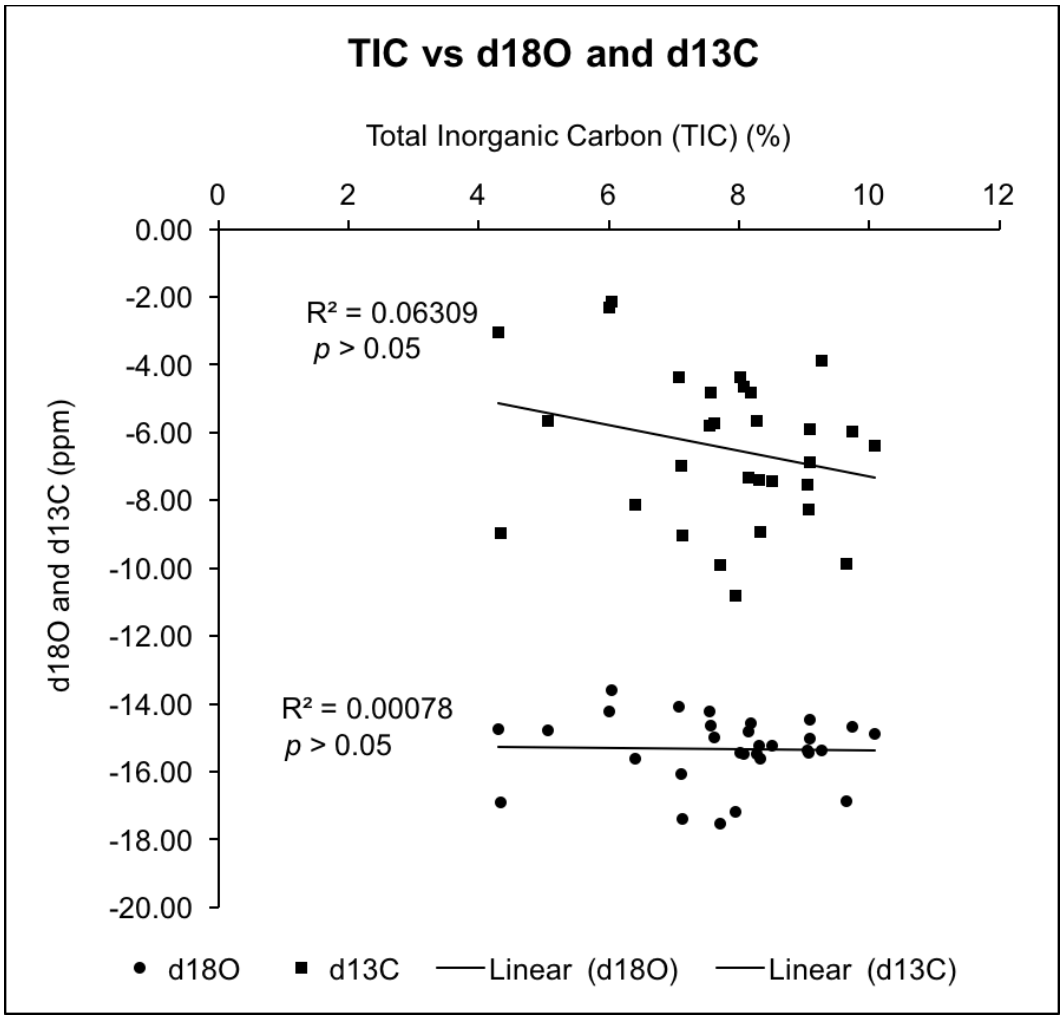

Figure 11. Correlations between percent total inorganic carbon (TIC) and $d^{18}O$ values (‰) and percent TIC and $d^{13}C$ values (‰) for 30 of the 51 samples analyzed for isotopes. Analysis revealed no significant correlation between TIC and $d^{18}O$ ($p > 0.05$; $R^2 = 0.00$), nor between TIC and $d^{13}C$ ($p > 0.05$; $R^2 = 0.06$).

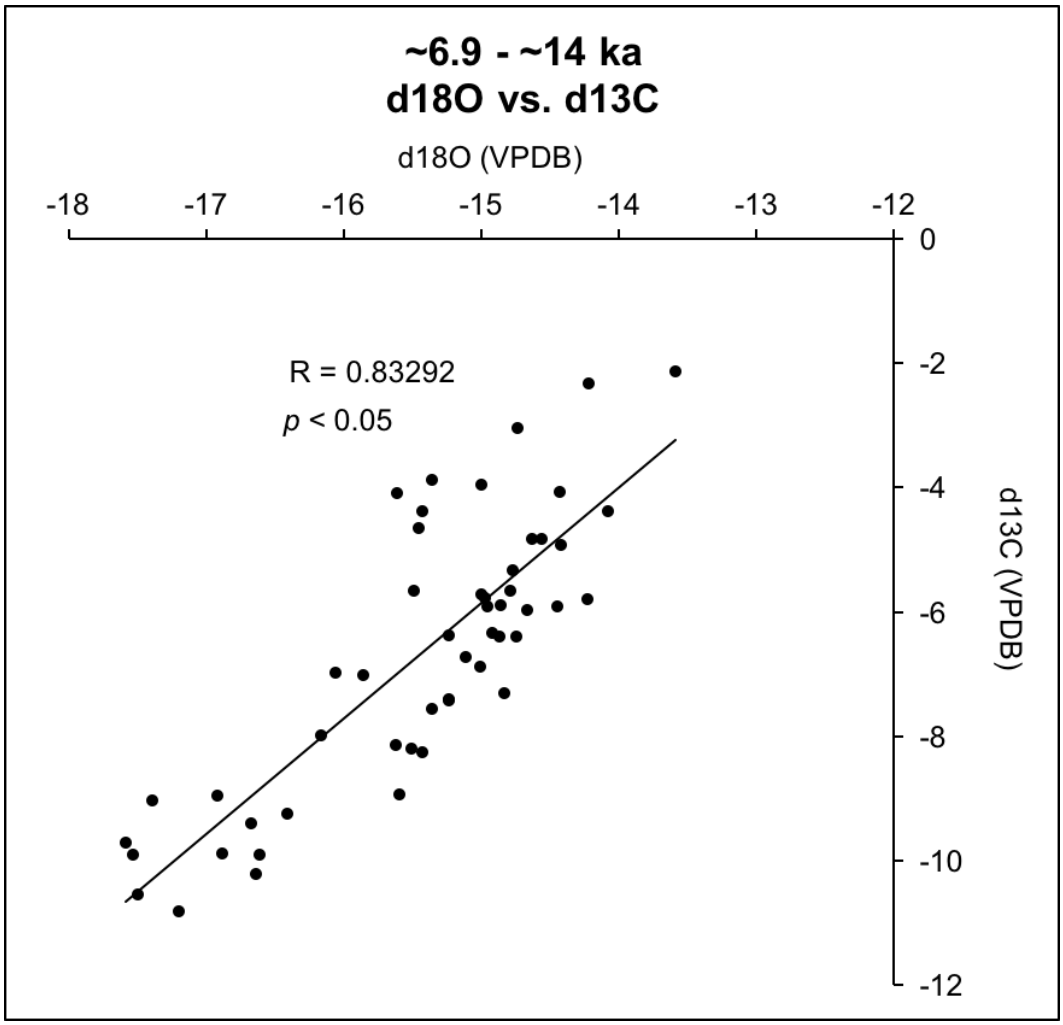

Figure 12. Correlation between $d^{18}O$ and $d^{13}C$ values during the late Pleistocene and early Holocene. $d^{18}O$ and the $d^{13}C$ values during the entire time-period analyzed here have a significant strong correlation (n = 51; $p < 0.05$; R= 0.83).

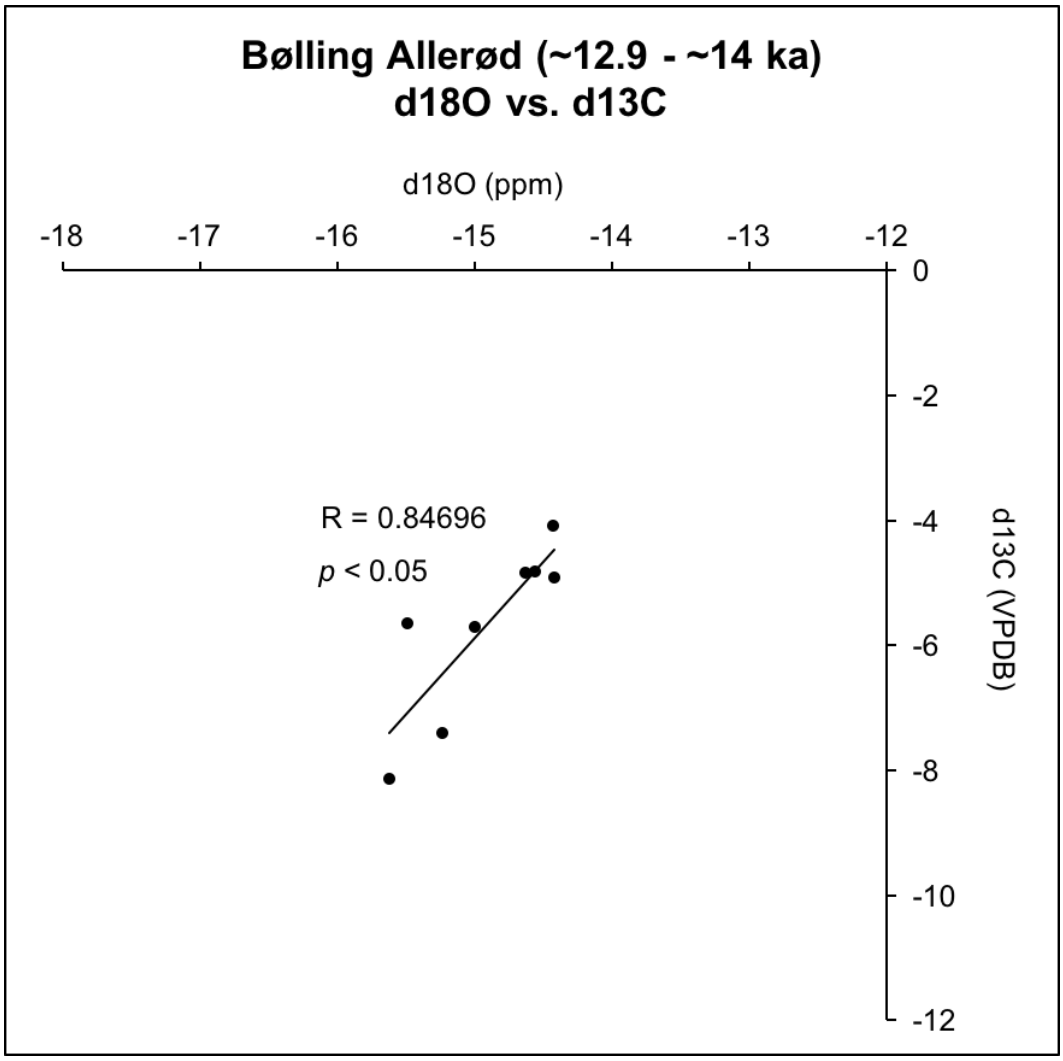

Figure 13. Correlation between $d^{18}O$ and $d^{13}C$ values during the Bølling Allerød (~12.9 - ~14 ka). $d^{18}O$ and $d^{13}C$ values during this interval yield a strong significant correlation (n = 8; $p < 0.05$; R = 0.85).

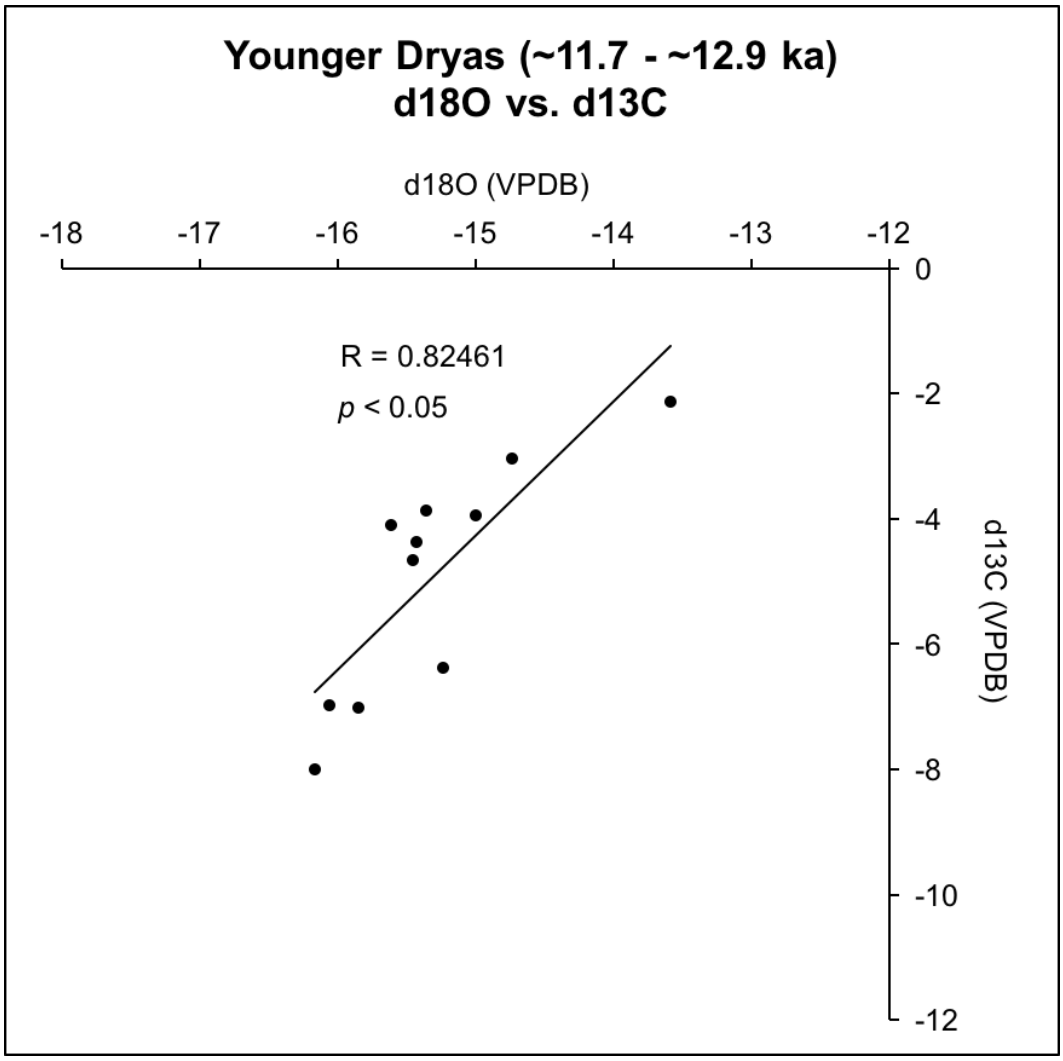

Figure 14. Correlation between $d^{18}O$ and $d^{13}C$ values during the Younger Dryas (~11-7- ~12.9 ka).$d^{18}O$ and $d^{13}C$ values during this climate interval have a significant strong correlation (n = 11; $p < 0.05$; R = 0.82).

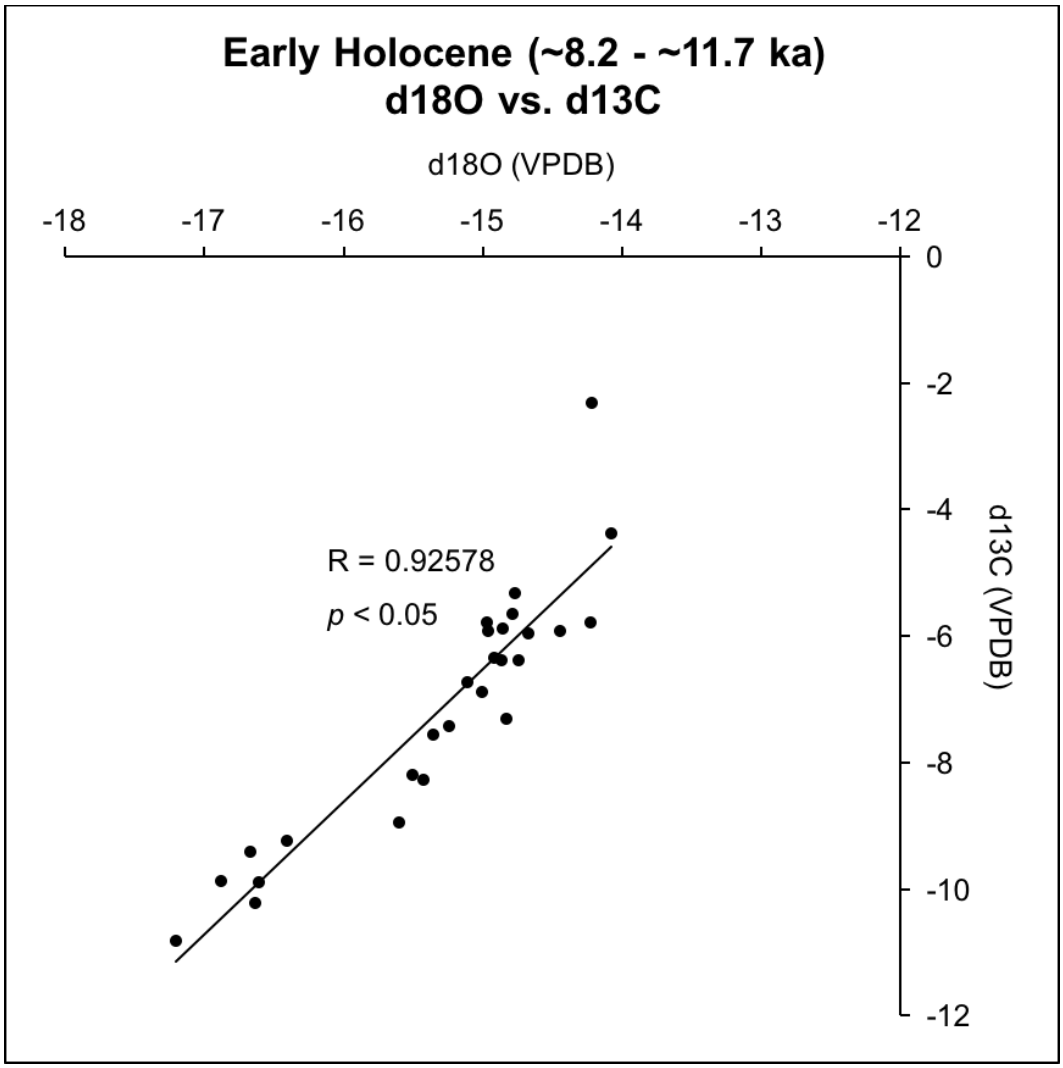

Figure 15. Correlation between $d^{18}O$ and $d^{13}C$ values during the Early Holocene (~8.2 - ~11.7 ka). $d^{18}O$ and $d^{13}C$ values during this climate interval have significant strong correlation (n = 27; $p < 0.05$; R = 0.93).

Tables

Stratigraphic Description	$CaCO_3$ content (%)	Sample ID
Yellow to white, spongey marl	68.2	6-85
	69.2	6-95
	75.5	4-82
	77.3	6-47
	81.2	5-66
	84.0	5-22
	Mean = 75.9	
Light brown, un-layered marl mud	58.9	5-78.5
	63.5	6-89
	69.0	7-39
	70.9	5-47
	75.5	5-11.5
	75.8	5-72
	Mean = 68.9	
Yellow marl with organic-rich laminations	59.3	6-67
	59.4	4-30
	64.3	4-7
	66.3	4-64
	66.7	6-40.5
	67.3	6-54
	69.3	5-39
	75.8	5-29
	80.4	4-70
	Mean = 67.64	
Glacial clay mixed with marl and organic material	63.0	7-57
Medium-brown, un-layered marl mud	42.2	4-51
	62.8	5-20
	67.8	4-95
	Mean = 57.6	
Organic matter evenly laminated with yellow marl	50.3	6-28
	53.4	7-46
	Mean = 51.9	
Dark gray to brownish-gray marl mud	35.9	6-21
	50.0	5-100
	Mean = 43.0	
Dark organic mud with flecks of yellow marl	36.1	4-24

Table 1. $CaCO_3$-containing samples organized by stratigraphic character. Respective $CaCO_3$ content (%) analyzed for the mean for each group.

Sample ID	Core Depth (cm)	Age (cal BP)	Stratigraphic Description	$CaCO_3$ content (%)
4-7	293	7401	Spongey, yellow marl with thin laminations of organic-rich mud	64.3
4-24	310	7835	Darker organic mud with specks of marl and dark brown organic matter	36.1
4-30	316	7992	Spongey, yellow marl with thin laminations of organic-rich mud	59.4
4-51	337	8521	Medium-brown marl mud	42.2
4-64	350	8846	Medium-brown marl mud with some thin, organic-rich laminations	66.2
4-70	356	8994	Light-brown to yellow, spongey marl with thin, organic-rich laminations	80.4
4-82	368	9294	Light-brown, un-layered marl mud	75.5
4-95	381	9619	Medium-brown, un-layered marl mud	67.8
5-11.5	395.5	9963	~0.5 cm-thick layer of yellow, spongey marl	75.6
5-20	404	10139	Medium-brown, un-layered marl mud	62.8
5-22	406	10175	Pure, yellow-white, spongey marl	84.0
5-29	413	10308	Light-brown, un-layered marl mud	75.8
5-39	423	10492	Medium-brown marl mud with dark organic-rich laminations	69.3
5-47	431	10638	Light-brown, un-layered marl mud	70.9
5-66	450	10996	Spongey, yellow marl with~2 mm layers of olive-green sediment	81.2
5-72	456	11104	Light-brown to yellow marl mud	75.8
5-78.5	462.5	11225.5	Light-brown marl mud	58.9
5-100	484	11582	Medium brownish-gray marl mud	50.0
6-21	498	11842	Dark grayish-brown marl mud	35.9
6-28	505	11969	Dark, organic-rich layers laminated with thin, yellow marl	50.3
6-40.5	517.5	12201.5	Spongey, yellow marl with thin, medium-brown layers	66.7
6-47	524	12322	Spongey, yellow, pure marl	77.3
6-54	531	12461	Light-brown marl mud with some thin layers of dark, organic-rich deposits	67.3
6-67	544	12747	Yellow marl laminated with dark, organic rich deposits	59.3
6-85	562	13163	Spongey, yellow marl	68.2
6-89	566	13254	Light-gray, spongey marl	63.5
6-95	572	13396	Yellow marl layered with light-gray marl	69.2
7-39	581	13605	Medium- to light-brown marl mud	69.0
7-46	588	13774	Darker organic-rich mud with very thin laminations of yellow marl	53.4
7-57	599	14029	Glacial clay mixed with marl and organic mud, layered with pure, yellow marl	63.0

Table 2. Sample ID, core depth, calibrated age, lithology, and calcium carbonate content for the 30 samples picked for isotope analysis.

Sample #	Lake	Core ID	BLF (cm)	Fraction Modern	±	$d^{14}C$ (‰)	±	^{14}C age (BP)	±	Graphite Mass (mg)	ABA completed	Identification notes
1	Kelly Lake	KLY18-4A-2	104	Not enough C to graphitize								
2	Kelly Lake	KLY18-4A-3	202	0.5793	0.0011	-425.4	1.1	4385	20	0.47	10/11/18	12 Alnus fruits, female Alnus catkin, spruce needle fragments
3	Kelly Lake	KLY18-4A-4	307.5	0.2326	0.0010	-769.3	1.0	11715	40	0.76	10/11/18	aquatic plant stem
4	Kelly Lake	KLY18-4A-5	295	0.3287	0.0011	-674.0	1.1	8940	30	0.51	10/11/18	wood fragments
5	Kelly Lake	KLY18-4A-6	433.5	0.2730	0.0013	-729.2	1.3	10430	40	0.33	10/11/18	terrestrial leaf fragments
6	Kelly Lake	KLY18-4A-7	554.5	0.2120	0.0010	-789.7	1.0	12460	40	0.58	10/11/18	wood fragments

Table 3. ^{14}C dating results and sample description.